Journal of Medicinal Chemistry

Article

Structural Modification of Natural Product Tanshinone I Leading to Discovery of Novel Nitrogen-Enriched Derivatives with Enhanced Anticancer Profile and Improved Drug-Like Properties

Chunyong Ding, Qianting Tian, Jie Li, Mingkun Jiao, Shanshan Song, Yingqing Wang, Ze-Hong Miao, and Ao Zhang

J. Med. Chem., **Just Accepted Manuscript** • DOI: 10.1021/acs.jmedchem.7b01259 • Publication Date (Web): 02 Jan 2018

ACS Publications

Journal of Medicinal Chemistry is published by the American Chemical Society. 1155 Sixteenth Street N.W., Washington, DC 20036

Structural Modification of Natural Product Tanshinone I Leading to Discovery of Novel Nitrogen-Enriched Derivatives with Enhanced Anticancer Profile and Improved Drug-Like Properties

Chunyong Ding,[†,§,#] Qianting Tian,[‡,§,#] Jie Li[†,∫], Mingkun Jiao,[†] Shanshan Song,[‡] Yingqing Wang,[*,‡,§] Zehong Miao[*,‡,§] and Ao Zhang[*,†,‡,∫,§]

[†]CAS Key Laboratory of Receptor Research, Synthetic Organic & Medicinal Chemistry Laboratory, Shanghai Institute of *Materia Medica*, Chinese Academy of Sciences, Shanghai 201203, China

[‡]State Key Laboratory of Drug Research, Shanghai Institute of *Materia Medica*, Chinese Academy of Sciences, Shanghai 201203, China

[∫]ShanghaiTech University, Shanghai 20120, China

§University of Chinese Academy of Sciences, Beijing 100049, China.

[#]These authors contributed equally to this work

[*]Correspondence and requests for materials should be addressed to A. Z. (email: aozhang@simm.ac.cn), Z. M. (email: zhmiao@simm.ac.cn), and Y. W. (email: yqwang@simm.ac.cn).

ABSTRACT

The clinical development of natural product tanshinone I (**1**) for cancer therapy is hampered by its weak potency and poor drug-like properties. Herein, a more broad and systemic structural modification on **1** was conducted to generate four series of new tanshinone derivatives. Among them, the lactam derivative **22h** demonstrated the most potent antiproliferative activity against KB and drug-resistant KB/VCR cancer cells, which are approximately 13- to 49-fold more potent than **1**. Compound **22h** possesses significantly improved drug-like properties including aqueous solubility (15.7 mg/mL), metabolic stability of liver microsomes, and PK characters ($T_{1/2}$ = 2.58 h; F = 21%) when compared to **1**. Preliminary mechanism studies showed that **22h** significantly induced apoptosis of HCT116 cells, at least partially, through activation of caspase-3/-7. More importantly, administration of **22h** at 10 mg/kg significantly suppressed the tumor growth of HCT116 xenograft *in vivo* without significant loss of body weight of the tested nude mice.

INTRODUCTION

The herbal medicine *Salvia miltiorrhiza* Bunge (Chinese name Danshen) is a well-known and widely used traditional Chinese medicine (TCM) for treating cardio- and cerebro-vascular diseases in Asian countries for centuries.[1] Both the hydrophilic (*e.g.* salvianolic acids) and the lipophilic components (*e.g.* tanshinones) are responsible for the cardiovascular actions of Danshen. In China, multiple composite formulas of Danshen have been awarded drug approval by the China Food and Drug Administration (CFDA). They are widely prescribed for treating cardiovascular disorders, especially atherosclerosis.[2a-b] Tanshinones, including tanshinone I (**1**, Tan-I), tanshinone IIA (**2**, Tan-IIA), and cryptotanshinone (**3**, CPT), represent a unique class of abietane-type *nor*-diterpenoid *ortho*-quinones that are exclusively isolated from Danshen, and show a wide spectrum of bioactivities, including antioxidative stress, anti-bacteria, anti-inflammation, anti-platelet aggregation, and anticancer (Figure 1).[2] Among the tanshinone class, **2** is the most widely investigated component due to its high content (~0.3%) in the herb. In contrast, **1** is less abundant, and has been relatively less studied. Previous studies have indicated that **1** is a potent anti-bacterial, anti-inflammatory, and learning and memory-enhancing agent.[2c, g-j] Particularly, its anticancer property has been more and more appreciated recently.[3] It was found that **1** significantly inhibited the growth of various cancer cells with low micromolar IC_{50} values by inducing cell cycle arrest and apoptosis.[4] Compound **1** was also reported to inhibit the migration, invasion, and metastasis of cancer cells through the alteration of matrix metalloproteinases. In addition, it has also been reported that **1** could overcome cancer multidrug resistance and inhibit tumor angiogenesis by reduction of phospho-705-Stat3.[5] Further, *in vivo* tumor growth inhibition was observed as well in several xenograft mice models.[6-7] Unfortunately, further

preclinical or clinical development of **1** as a new antitumor therapeutic agent has been dampened by its weak potency, extremely low aqueous solubility (<10^{-4} mg/mL),[8] and poor PK properties ($T_{1/2}$ = 0.17 h; *F* = ~0%).[9] Therefore, structural modification on **1** aiming at promoting both the antitumor efficacy and the drug-like properties is highly needed.

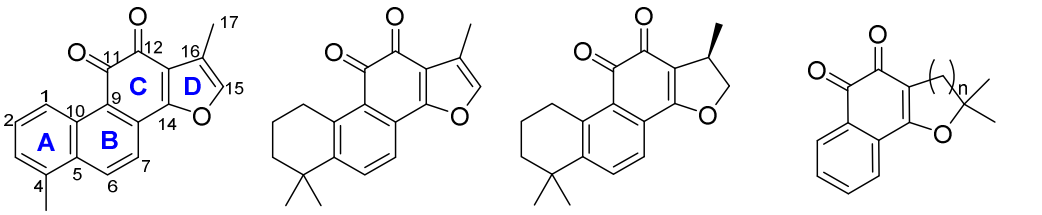

Figure 1. Structures of representative tanshinones (**1-3**) and lapachone compounds (**4-5**)

Structurally, tetracyclic **1** contains naphthalene rings A and B, *ortho*-quinone C, and furan ring D. Compared to structures **2** and **3**, **1** is much less drug-like due to its larger planar aromatic tetracyclic scaffold, and has limited sites for structural modification. Previously, a limited number of structural modifications have been reported (Figure 2), including introduction of some moieties (carboxylic acid, amine, or alcohol)[10] that help to increase water solubility as an appendage at C-15, simple alkyl substitution on the ring A[11] or masking the *ortho*-quinone moiety to form an imidazole ring[12]. However, most of these analogues still suffered from modest *in vitro* antitumor efficacy and unsatisfactory PK properties, which justify an urgent need for conducting a more broad and systemic structural modification on **1** to develop novel tanshinone analogues not only with elevated antitumor efficacy but also with improved drug-like properties including aqueous solubility, metabolic stability, and

PK properties. To this end, in this manuscript we designed four series of tanshinone analogues (Figure 1), including: 1) introducing diversified nitrogen-containing functional groups at C-17 to increase both aqueous solubility and molecular flexibility (**Series 1**); 2) dearomatizing the metabolically unstable furyl ring both to increase the molecular stability and to reduce the aromaticity of **1** that may improve the physico-chemical property (**Series 2**); 3) replacing the naphthylene A/B ring with isoquinolinone (**Series 3**) or isoquinoline (**Series 4**) to modify the middle B ring both to reduce the lipophilicity and to anchor a side chain on the *N*- or *O*-moiety that helps to increase aqueous solubility. Herein, we describe the synthesis and pharmacological investigation of these new series of tanshinone analogues.

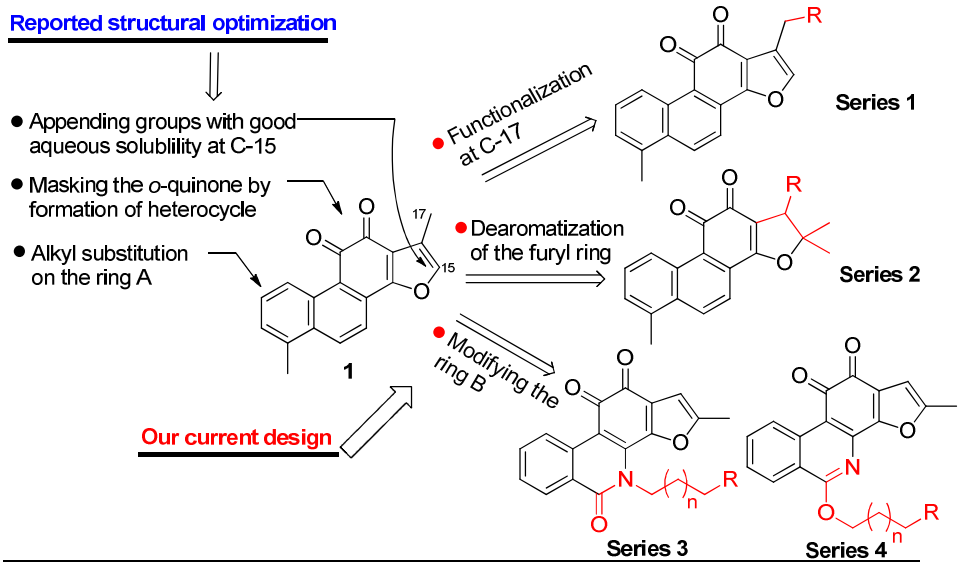

Figure 2. Reported structural optimization and our new design (**series 1-4**)

RESULTS AND DISCUSSIONS

The chemical modification at the furan methyl group of **1** was barely reported due to its relatively low reactivity. First, we synthesized the 17-hydroxylated tanshinone **6**[13] (przewatanshinquinone B), which is also a natural product isolated from *Salvia*

miltiorrhiza in the early 1980s. As shown in Scheme 1, refluxing of **1** in dioxane/H_2O using SeO_2 as the oxidant selectively gave rise to **6** as the sole product in 26% yield with recovered **1** in 45% yield. Subsequent bromination of **6** with PBr_3 in dichloromethane afforded 17-bromo intermediate **7** in 56% yield, which was further reacted with various acyclic and cyclic alkyl amines to give a series of 17-amino products **8a-o** in 46-95% yields.

Scheme 1. Synthesis of Compounds **6** and **8a-o**[a]

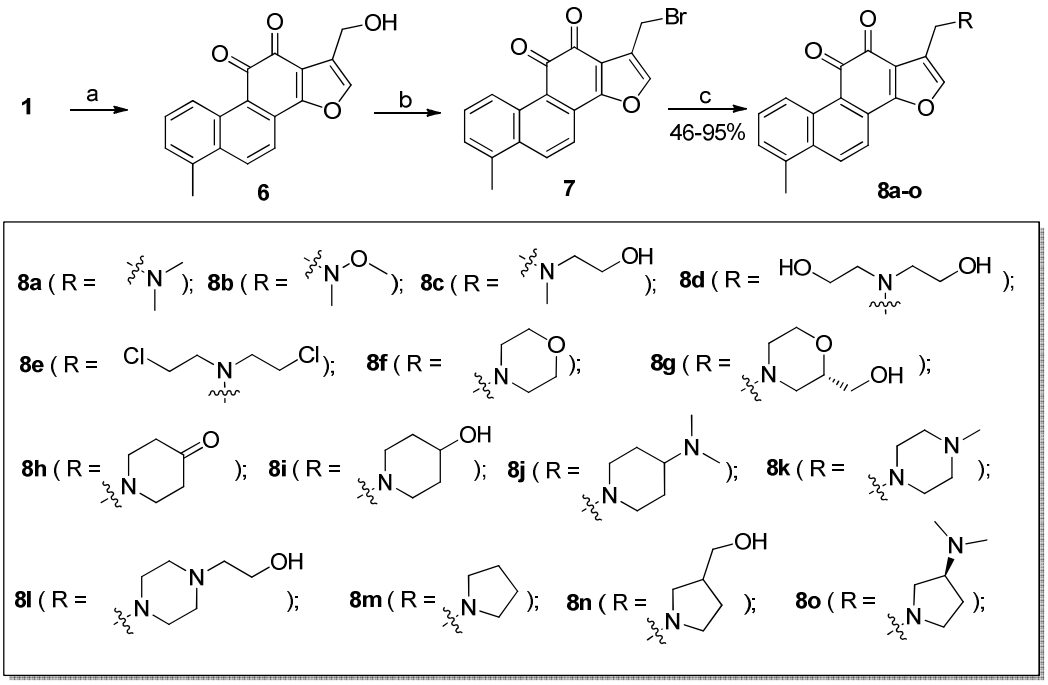

[a]Reaction condition and reagents: a) SeO_2, 1,4-dioxane/H_2O, 100 °C, 26%; b) PBr_3, DCM, 56%; c) Secondary alkyl amines, K_2CO_3, DCM/CH_3CN, rt.

Scheme 2. Synthesis of derivatives **11-13** and **14a-b**[a]

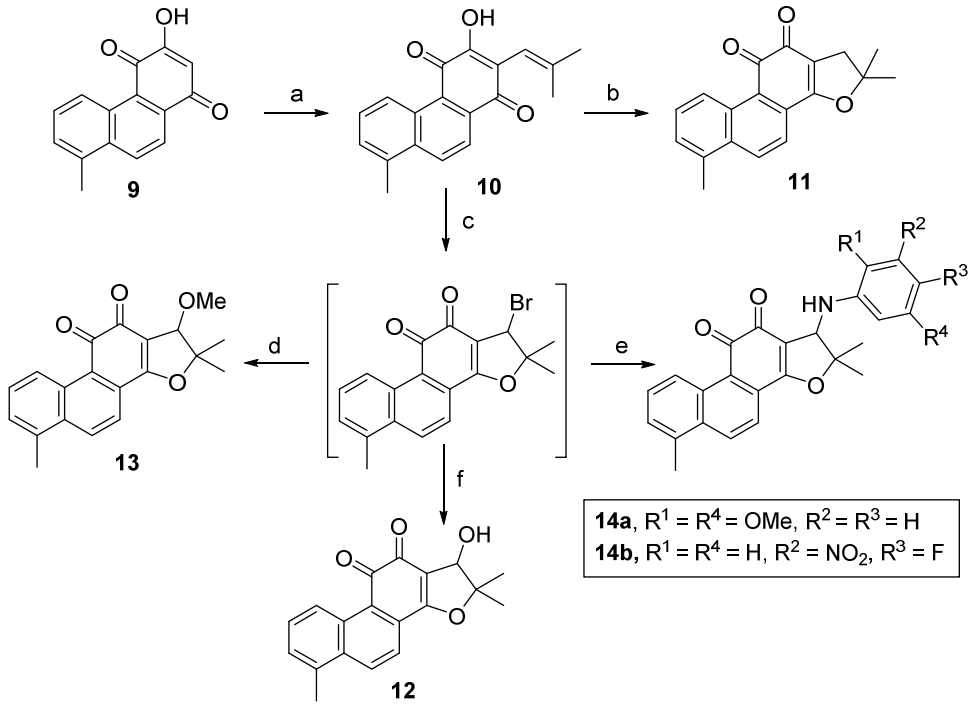

[a]Reaction conditions and reagents: a) Isobutyraldehyde, CH_3NH_2HCl, *p*-TsOH, 105 °C, 94%; b) $AlCl_3$, DCM, rt, 72%; c) Br_2, DCM, rt; d) MeOH, rt, 40%; e) Substituted anilines, DCM, rt, 59-60%; f) H_2O, THF, 63%.

Inspired by the dihydrofuran structure of nor-*β*-lapachone (**4**), a well-documented anticancer drug candidate,[14] a series of dihydrofuran derivatives with reduced aromaticity were designed and synthesized. As described in Scheme 2, the synthesis commenced with 3-hydroxyphenanthrene-1,4-dione **9**[11b], a key intermediate in our previously reported total synthesis of **1**. The preparation of intermediate **10** was achieved in 94% yield by using a similar literature protocol,[15] which involved a Mannich reaction of **9** with isobutyraldehyde and methanamine hydrochloride followed by elimination with *p*-toluenesulfonic acid in refluxing toluene. Subsequently, compound **10** further underwent $AlCl_3$-catalyzed cyclization to give dihydrofuran product **11** in 72% yield. Similar to a literature procedure,[14]

treatment of **10** with bromine in dichloromethane provided a highly reactive 16-bromo intermediate, which was reacted with saturated $NaHCO_3$ aqueous solution without further purification to afford 16-hydroxyl product **12** in 63% yield. Likewise, treating the intermediate with anhydrous methanol or various anilines yielded 16-methoxyl product **13** in 40% yield and a series of 16-arylamino derivatives **14a-b** in moderate yields.

Scheme 3. Synthesis of compounds **20a-e**[a].

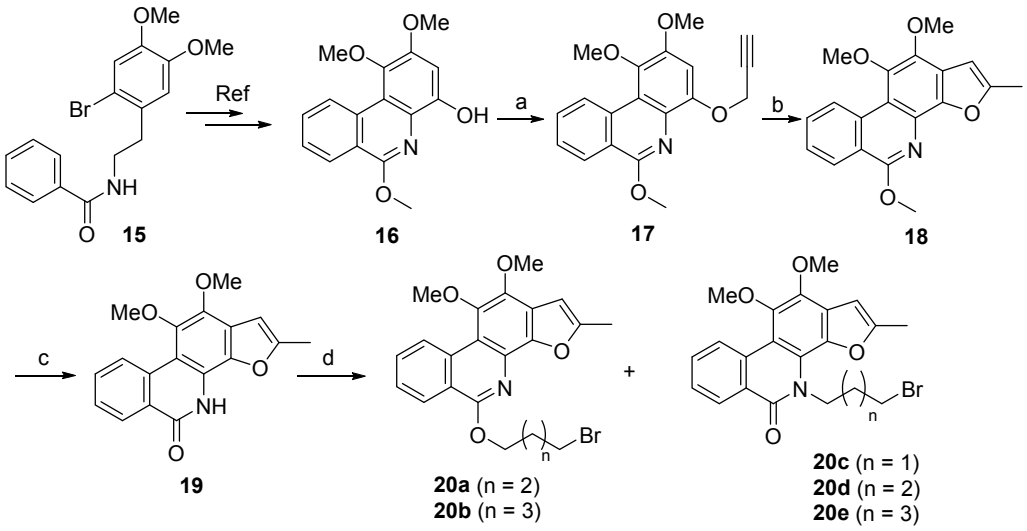

[a] Reaction conditions and reagents: a) 3-Bromopropyne, K_2CO_3, acetone, 60 °C, 98%; b) CsF, DEA, 200 °C, 69%; c) Iodotrimethylsilane, NaI, DCM, rt, 98%; d) 1,3-Dibromopropane, K_2CO_3, DMF, 80 °C, 20-69%;

Structural modification on the B-ring of **1** has never been explored so far. Inspired by the anticancer potential of indenoisoquinoline analogues,[16] a series of 7-aza derivatives of **1** were designed and synthesized. As described in Schemes 3-5, the synthesis commenced from the phenol intermediate **16**, which was prepared from the bromo amide **15** according to a literature procedure.[17] Treating **16** with propargyl bromide in the presence of K_2CO_3 followed by CsF-assisted cyclization in refluxing $PhNEt_2$ gave the furan product **18** in 69% yield, which was then desmethylated by

trimethylsilyl iodide (TMSI) to provide lactam **19** in a quantitative yield. Alkylation of **19** with 1,4-dibromobutane in the presence of K_2CO_3 yielded *O*- and *N*-alkylated products **20a** and **20d** in 20% and 28% yields, respectively. Their structures could be discriminated by heteronuclear multiple bond correlation (HMBC) NMR as described in Figure 1S (SI). Similarly, alkylation of **19** with 1,5-dibromopentane under the same condition also gave *O*- and *N*-alkylated products **20b** and **20e** in 24% and 33% yield, respectively. Interestingly, when 1,3-dibromopropane was used, only *N*-alkylated product **20c** was obtained in 69% yield (Scheme 3). *O*-Desmethylation of compounds **20a-e** with BBr_3 afforded *o*-quinone intermediates **21a-e** in 60-98% yields, which were further aminated with various secondary amines to furnish a series of *N*-aminoalkyl *o*-quinones **22a-m** in 44-88% yields (Scheme 4).

Scheme 4. Synthesis of compounds **22a-m**[a].

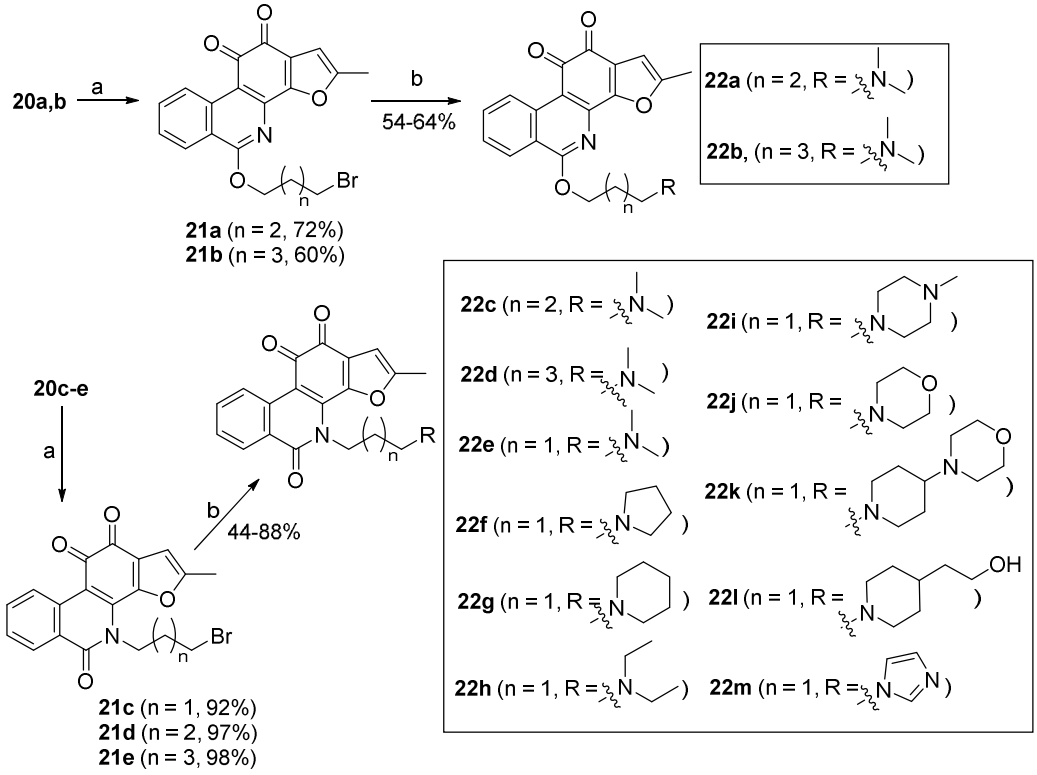

[a] Reaction conditions and reagents: a) BBr_3, THF, -78 °C to rt; b) Secondary alkyl amines, K_2CO_3, DMF.

As depicted in Scheme 5, alkylation of **19** with 1-bromo-2-(2-bromoethoxy)ethane produced *N*- and *O*-alkylated products **20f** and **20g** in 43% and 39% yields, respectively. *O*-Desmethylation of **20f** with BBr_3 led to the cleavage of the *N*-oza-alky side chain and provided *N*-ethanol quinone **21f** in 29% yield. *O*-Desmethylation of **20g** with BBr_3 produced the desired quinone **21h** in 71% yield together with *O*-hydroxyethyl **21g** as the side product. Treating **21h** with dimethylamine hydrochloride in the presence of K_2CO_3 smoothly delivered the aminated products **22n** in 35% yield.

Scheme 5. Synthesis of compounds **21f-g** and **22n**[a]

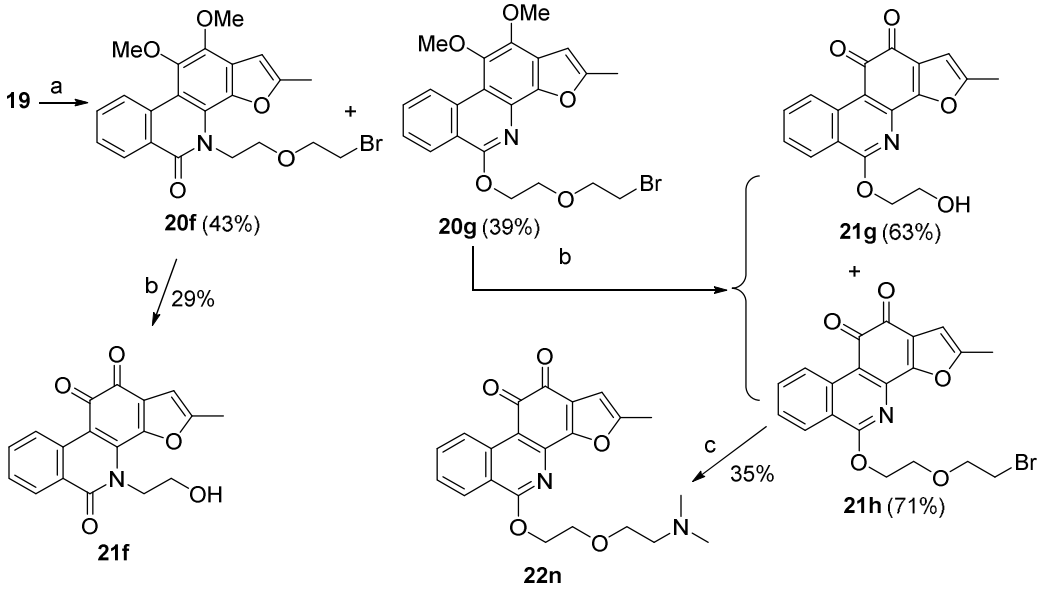

[a] Reaction conditions and reagents: a) 1,3-Dibromopropane, K_2CO_3, DMF, 80 °C; b) BBr_3, THF, -78 °C; c) dimethylamine, K_2CO_3, DMF.

***In vitro* antiproliferative activity.** The growth inhibitory effects of all the synthesized derivatives of **1** were evaluated against a pair of human cancer cell lines, *i.e.* squamous carcinoma KB cells and the corresponding vincristine-resistant KB/VCR cells，by sulforhodamine B (SRB) assays as described in the *in vitro* screening protocol (Experimental Section). The results are summarized in Tables 1-3.

Both **1** and the anticancer drug vincristine (VCR) were chosen as positive controls. As described in Table 1, 17-hydroxyl compound **6** exhibited more potent antiproliferative effects against two tested cancer cell lines when compared to **1**. Most of 17-amino compounds not only exhibited significantly improved antiproliferative activity against KB cells, but also displayed marked growth inhibitory effects against vincristine-resistant KB/VCR cells. In the series of 17-amino derivatives **8a-o**, dimethylamino compound **8a** displayed the most potent antiproliferative activity against two tested cancer cell lines with IC_{50} values of 1.11 μM and 0.51 μM, respectively. The *N*,*O*-dimethylhydroxylamino derivative **8b** showed a decreased potency with IC_{50} values greater than 5 μM, and the amino derivatives **8c-d** with terminal hydroxyl groups exhibited comparable antiproliferative activity with IC_{50} values around 1.0 μM, while removal of the terminal hydroxyl in **8e** resulted in less potent activity, indicating the hydroxyl group was critical for the potency. Although 17-morpholino derivative **8f** displayed very weak antiproliferative activity with IC_{50} values greater than 20 μM, the anticancer activity could be significantly boosted when the hydroxymethyl group was introduced in the morpholinyl ring (compound **8g**). The similar tendency was also observed in the series of 17-piperidinyl, -piperazinyl, and -pyrrolidinyl derivatives. For instance, replacement of 4-ketone of the piperidine ring (compound **8h**) with aqueous hydroxyl or amino groups led to derivatives **8i-j** with significantly increased potency against two tested cancer cells. 17-Piperazinyl derivative **8k** displayed less potent anticancer activity against KB and KB/VCR cells than 17-Piperazine derivative **8l** with a terminal hydroxyl group. 17-Pyrrolidinyl

derivative **8m** was found possessing potent inhibitory activity with IC_{50} values of 1.59 μM and 1.79 μM, respectively. Further installation of dimethylamino or hydroxyl groups in the pyrrolidinyl ring displayed the comparable activity (**8n-o**). These results indicate introduction of the amino or hydroxyl moieties with good aqueous solubility at C-17 is beneficial for the anticancer activity.

Table 1. Antiproliferative effects of 17-modified derivatives against human cancer cell lines[a]

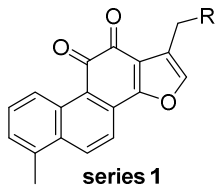

series 1

Compd #	R	IC_{50} (μM)	
		KB	KB/VCR
6	OH	3.22 ± 0.65	2.95 ± 0.69
8a		1.11 ± 0.30	0.51 ± 0.03
8b		8.12 ± 3.19	5.71 ± 1.55
8c	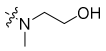	1.50 ± 0.09	1.02 ± 0.07
8d	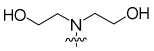	1.64 ± 0.30	1.43 ± 0.06
8e	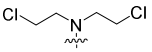	9.43 ± 6.18	10.88 ± 4.84
8f		＞20	＞20
8g	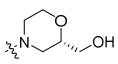	4.97 ± 3.01	2.41 ± 0.15
8h		9.71 ± 4.88	4.74 ± 0.23
8i	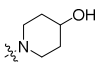	1.54 ± 0.31	1.11 ± 0.14
8j	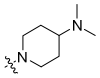	3.80 ± 0.40	3.82 ± 0.08
8k		5.22 ± 0.77	13.12 ± 1.23

8l	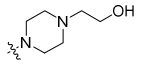	2.68 ± 0.26	4.41 ± 0.02
8m		1.59 ± 0.16	1.79 ± 0.25
8n		1.27 ± 0.26	0.91 ± 0.21
8o		2.61 ± 0.08	1.70 ± 0.03
1	-	5.87 ± 0.70	4.40 ± 0.12
VCR (nM)	-	0.72 ± 0.16	357.51 ± 29.89

[a]IC_{50} values are shown as the mean ± SEM (μM) from two independent experiments.

Among the furyl ring-dearomatized analogues (Table 2), dihydrofuran **11** exhibited moderate inhibitory activity against the proliferation of the two tested cancer cells with IC_{50} values around 2.0 μM. Installation of the hydroxyl group at the *β*-position of the furan ring afforded 16-hydroxyl derivative **12** displaying enhanced potency with IC_{50} values of 1.63 μM and 1.24 μM, respectively. 16-Methoxyl dihydrofuran derivative **13** exhibited marginally less potent activity than **12**. However, anilines-substituted derivatives **14a-b** were found to be completely inactive with IC_{50} values greater than 20 μM, probably due to the increased hydrophobicity.

Table 2. Antiproliferative activity of dihydrofuran derivatives against human cancer cells[a]

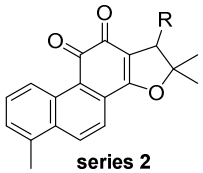

series 2

Compd #	R	IC_{50} (μM)	
		KB	KB/VCR
11	H	2.62 ± 0.23	2.37 ± 0.01
12	OH	1.63 ± 0.03	1.24 ± 0.23

13	OMe	2.19 ± 0.49	2.02 ± 0.76
14a	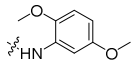	＞20	＞20
14b	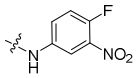	＞20	＞20
1	-	5.87 ± 0.70	4.40 ± 0.12
VCR (nM)	-	0.72 ± 0.16	357.51 ± 29.89

[a]IC_{50} values are shown as the mean ± SEM (μM) from two independent experiments.

In the series of 7-aza derivatives with various alkyl side chains, significant discrepancy in the cellular potency was observed (Table 3). *N*- or *O*-hydroxyethyl derivatives **21f** and **21g** were completely inactive with IC_{50} values greater than 20 μM. *N*-3-(Dimethylamino)propyl derivative **22e** showed significant boost in potency with IC_{50} values of 0.71 μM and 0.92 μM, respectively. Extending the length of *N*- or *O*-alkyl side chain led to decreased cellular potency, especially for KB cells. For example, *O*-3-(dimethylamino)butyl derivative **22a** displayed much weaker activity with IC_{50} values greater than 20 μM. In contrast, *N*-3-(dimethylamino)butyl derivative **22c** possessed moderate antiproliferative activities with IC_{50} values of 4.05 μM and 2.47 μM, respectively. *O*- or *N*-aminopentyl derivatives **22b** and **22d** exhibited about 2- to 7-fold more potent inhibitory activity against KB/VCR cells than KB cells, indicating great potential for overcoming cancer drug resistance. Interestingly, replacement of the middle carbon of the *O*-aminopentyl side chain of **22b** with oxygen led to the oxa derivatives **22n** partially recovering the potency against KB cells with IC_{50} values of 3.78 μM, while their potency against KB/VCR cells was still retained. Taking together, *N*-aminopropyl side chain was identified to be the optimal one attached to the 7-aza B-ring. Next, another series of derivatives **22f-m** with

various *N*-aminopropyl side chains were further evaluated against the growth of KB and KB/VCR cells. As shown in Table 3, most of them exhibited potent antiproliferative activity with low micromolar or submicromolar IC_{50} values. Among them, *N*-3-(diethylamino)propyl derivative **22h** displayed the most potent antiproliferative activity against all tested cancer cells with IC_{50} values of 0.12 μM (KB) and 0.33 μM (KB/VCR), respectively. Replacement of the diethylamino group of **22h** with various cyclic amino groups, such as pyrrolidinyl (**22f**), piperidinyl (**22g**), 4-methylpiperazin-1-yl (**22i**), morpholino (**22j**), and imidazolyl (**22m**), decreased the potency. Further modifications on the piperidine ring failed to improve the inhibitory activity (**22k-l**) as well. As thus, compound **22h** was identified as the most potent natural product derivative deserving further study.

Table 3. Antiproliferative activity of 7-aza derivatives with different *N*- or *O*-alkyl chains[a]

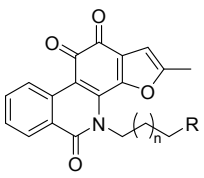

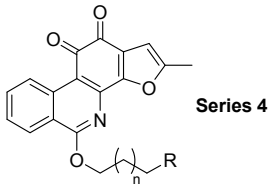

Compd #	Series	n	R	IC_{50} (μM)	
				KB	KB/VCR
21f	3	0	OH	＞20	＞20
21g	4	0	OH	＞20	＞20
22a	4	2	NMe_2	＞20	＞20
22b	4	3	NMe_2	15.27 ± 0.10	1.99 ± 0.25
22c	3	2	NMe_2	4.05 ± 0.05	2.47 ± 0.78
22d	3	3	NMe_2	13.84 ± 1.37	5.17 ± 0.69
22e	3	1	NMe_2	0.71 ± 0.16	0.92 ± 0.02

22f	3	1		3.40 ± 078	2.64 ± 1.07
22g	3	1		1.12 ± 0.49	1.53 ± 0.70
22h	3	1	NEt_2	0.12 ± 0.02	0.33 ± 0.04
22i	3	1		10.38 ± 3.43	3.52 ± 0.99
22j	3	1		2.30 ± 0.54	1.56 ± 0.65
22k	3	1	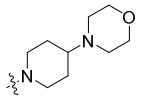	0.34 ± 0.22	1.72 ± 0.65
22l	3	1	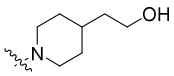	0.87 ± 0.11	1.49 ± 0.02
22m	3	1		17.24 ± 1.72	10.07 ± 4.56
22n	4	0	$OCH_2CH_2NMe_2$	3.78 ± 1.23	1.65 ± 0.01
1	-	-	-	5.87 ± 0.70	4.40 ± 0.12
VCR (nM)	-	-	-	0.72 ± 0.16	357.51 ± 29.89

[a]IC_{50} values are shown as the mean ± SEM (μM) from two independent experiments.

Aqueous Solubility. To investigate whether the synthesized derivatives possess better aqueous solubility than **1**, a literature reported High Performance Liquid Chromatography (HPLC) method[18] was employed to measure the solubility of several selected analogues with significantly improved anticancer activity, including **8a**, **12**, and **22h**. One-point calibration was conducted against standards with known concentrations of sample compounds to determine concentrations of the indicated compounds. As expected, these compounds bearing hydroxyl or amino groups not only have enhanced anti-proliferative activity but also possess significantly improved aqueous solubility. For instance, aqueous solubility of **12** bearing a 16-hydroxyl dihydrofuran moiety was determined to be 0.09 ± 0.02 mg/mL, and the solubility of

the amino derivatives **8a** (HCl salt) and **22h** (free base) were 8.03 ± 0.42 mg/mL and 15.74 ± 0.60 mg/mL, respectively (Figure 3). In addition, the amino compound **22h** in the form of HCl salt possess a superior aqueous solubility greater than 80 mg/mL. In contrast, the aqueous solubility of **1** was too low to be determined by this method ($<10^{-4}$ mg/mL in literature[8]).

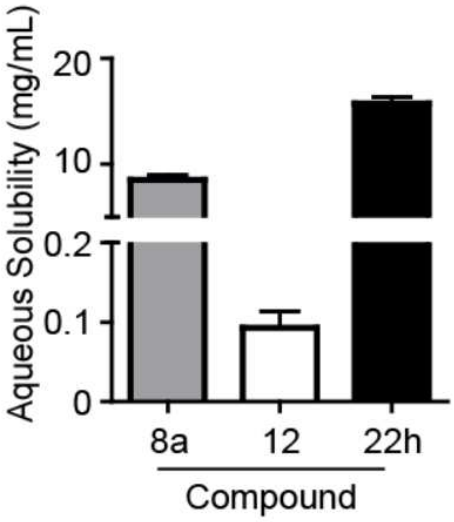

Figure 3. Aqueous solubility of compounds **8a** (HCl salt), **12**, and **22h**. The values are the mean ± SD of at least three independent experiments.

***In Vitro* Metabolic Stability Assessment.** *In vitro* metabolic stability of compounds **8a**, **12**, and **22h** was assessed in liver microsomes of human, rat, and mouse, respectively. As shown in Table 6, compared to **1**, all of these compounds possessed markedly improved metabolic stability in all tested microsomes with about 8- to 78-fold longer plasma half-time ($T_{1/2}$) and lower intrinsic clearance (Clint). Interestingly, these new derivatives were more stable in human liver microsomes than in the other species. Particularly, compound **8a** demonstrated the superior stability in human liver microsomes with $T_{1/2}$ of 501 min and lower clearance (Clint, 4.19 mL/min/g protein). In general, compound **22h** displayed much improved stability

across all the tested microsomes.

Table 6. *In Vitro* Metabolic Stability in Liver Microsomes.

Compound	Species	$T_{1/2}$ (min)	Clint In Vitro (mL/min/g protein)
1	Human	6.45	325.42
	Rat	2.51	835.82
	Mouse	-[a]	-[a]
8a	Human	501.06	4.19
	Rat	22.66	92.68
	Mouse	40.66	51.65
12	Human	57.10	36.79
	Rat	20.17	104.12
	Mouse	25.29	83.07
22h	Human	89.46	23.48
	Rat	75.81	27.71
	Mouse	54.53	38.52

[a]The values cannot be determined due to the extreme instability.

***In Vivo* Pharmacokinetic (PK) Study of Compound 22h**. To explore the further developability of the new identified tanshinone derivatives, compound **22h** was further evaluated for its pharmacokinetic properties in male SD rats after intravenous and oral administration, respectively. As shown in Table 7, compound **22h** given orally at 3 mg/kg displayed a half-life ($T_{1/2}$) of 2.58 h, a peak plasma concentration (C_{max}) of 33.7 ng/mL, and an AUC value of 81.4 h*ng/mL. Besides, compound **22h** showed an oral bioavailability of 21.0%. Taken together, compared to the poor PK of the natural product **1** with short $T_{1/2}$ (0.17 h) and low oral bioavailability (~0%)[9], compound **22h** exhibited significant improvements on overall PK properties.

Table 7. Preliminary Pharmacokinetic Parameters for Compound **22h**[a-d]

		$T_{1/2}$ (h)	T_{max} (h)	C_{max} (ng/mL)	AUC (h*ng/mL)	$CL_{\_obs}$ (mL/min/kg)	MRT_{INF_obs} (h)	$Vss_{\_obs}$ (mL/kg)	*F* (%)
22h	*po*	2.58	0.25	33.7	81.4	-[e]	3.72	-[e]	21.0
	iv	1.51	-[e]	-[e]	114	176	0.835	7980	-[e]

[a]Values are the average of three runs; Vehicle: DMSO, Tween 80, normal saline. CL, clearance; Vss, volume of distribution; $T_{1/2}$, half-life; C_{max}, maximum concentration; T_{max}, time of maximum concentration; MRT, mean residence time; AUC, area under the plasma concentration time curve; *F*, oral bioavailability. [b]Dose: p.o. at 3.0 mg/kg; [c]Dose: i.v. at 1.0 mg/kg; [e]Not determined.

Compound 22h Elicited Broad-Spectrum *In Vitro* Antitumor Effects. To further characterize the anticancer activity of the most promising compound **22h**, it was tested against a panel of eight human cancer cell lines, including lung (A549, H460), colon (HCT116), breast (BT-474), prostatic (DU-145), hepatoma (HepG, BEL7404), and gastric (MGC803) cancer cells, as well as normal human umbilical vein endothelial cells (HUVEC) as the control. As shown in Table 8, compound **22h** exhibited the similar *in vitro* anticancer activity with IC_{50} values ranging from 0.14 to 1.31 μM against all of the tested human cancer cell lines, and the activity against HUVEC was relatively less potent. The results indicated that the lactam derivative **22h** possessed a relatively broad spectrum of antitumor activity.

Table 8. Inhibitory Effect of **22h** against Proliferation of Various Cancer Cells.[a]

	IC_{50} (μM)								
	HUVEC	A549	HCT116	MGC803	HepG	BEL7404	DU-145	BT-474	H460
22h	2.52 ± 0.63	0.19 ± 0.05	0.14 ± 0.03	0.26 ± 0.08	1.31 ± 0.32	0.36 ± 0.11	0.22 ± 0.04	0.77 ± 0.23	0.17 ± 0.02

[a]IC_{50} values are shown as the mean ± SD (μM) from three separate experiments.

Compound 22h Induced Apoptosis of HCT116 Cells. To determine whether the

proliferative inhibition induced by **22h** in HCT116 cells was attributed to apoptosis, HCT116 cells were treated with vehicle and compound **1** in parallel with **22h** at different concentrations (0.5, 1.0, or 2.0 μM) for 48 h, and then stained with FITC-Annexin V-FITC and propidium iodide (PI). The percentages of apoptotic HCT116 cells were determined by flow cytometry. As shown in Figure 4, compound **22h** displayed moderate effects to induce apoptosis of HCT116 cells in a concentration-dependent manner, resulting in 6.6%, 17.7%, and 56.6% of apoptotic cells (early and late apoptosis) at 0.5 μM, 1.0 μM, and 2.0 μM, respectively, as compared to 9.3% of compound **1** at 2.0 μM. Apparently, **22h**-induced apoptosis of HCT116 cells, at least in part, contributes to its antiproliferative effects. Interestingly, when the cells were pretreated with pan-caspase inhibitor Z-VAD-FMK (a pan-caspase inhibitor)[19] at 20 μM, compound **22h** displayed a decreased potential to induce the apoptosis, resulting in 5.6%, 9.5%, and 34.4% of apoptotic cells (early and late apoptosis) at the same concentrations as above, respectively. The result indicated that the apoptosis induced by **22h** is partially ascribed to the caspase activation.

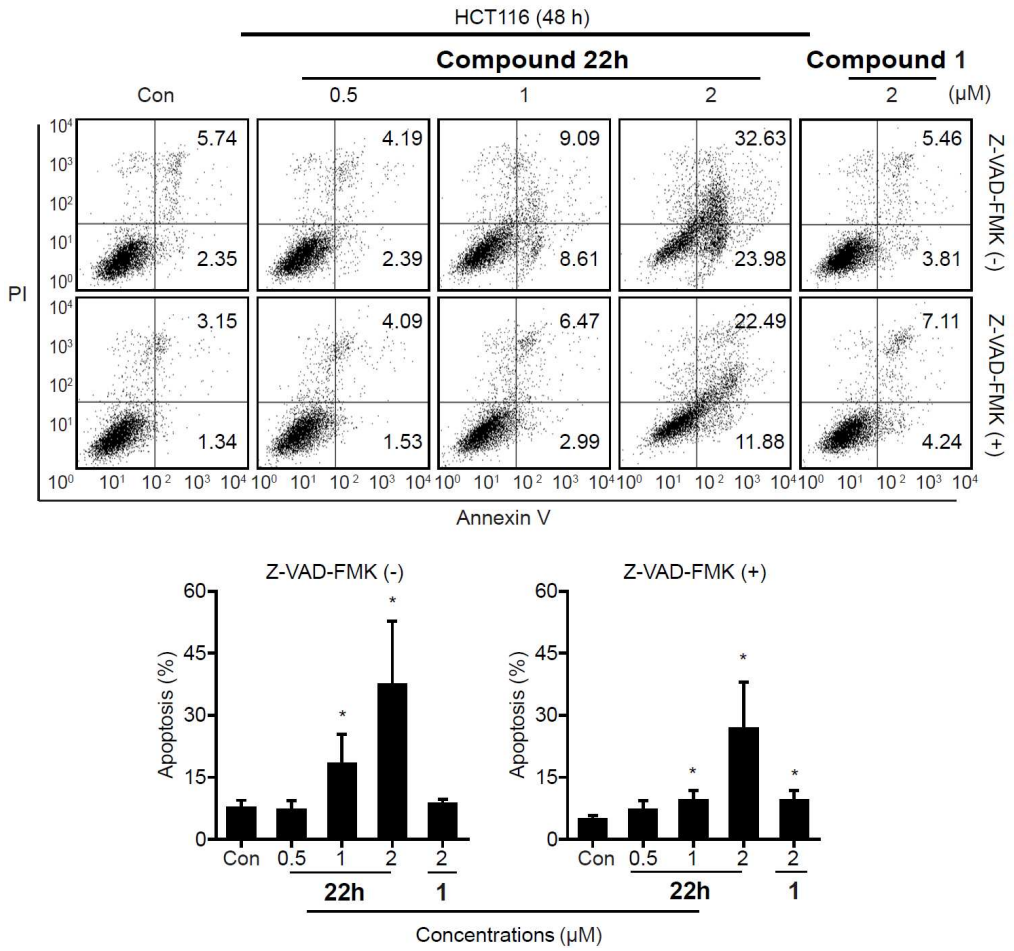

Figure 4. Apoptosis induced by **22h** or **1** at different concentrations in HCT116 cells pretreated with or without 20 μM Z-VAD-FMK for 1 h was analyzed by Annexin V-FITC/PI-staining-based flow cytometry. Upper: representative images; lower: data from three separate experiments expressed as mean ± SD. Data were analyzed by Student *t* test. *, $p < 0.05$.

Effects of 22h on Apoptosis-Related Proteins PARP and Caspase 3/7. To further elucidate the potential mechanisms contributed to the apoptotic induction by compound **22h**, several proteins as markers of apoptosis were determined by Western blotting. As shown in Figure 5, treatment of HCT116 cells with **22h** at low concentrations (0.5 - 2 μM) triggered cleavage of PARP and caspase 3/7 as indicated

by the appearance of PARP fragments and activated caspase 3/7 in a concentration-dependent manner, which could be reversed by pretreatment with Z-VAD-FMK (20 μM) for 1 h. However, compound **1** failed to induce the cleavage of PARP and caspase 3/ 7 to their activated forms at 2 μM in HCT116 cells pretreated with or without 20 μM Z-VAD-FMK. In addition, **22h** could significantly improve the caspase 3/7 activity in HCT116 cells at the concentrations ranging from 1.0 μM to 4.0 μM (Figure 6). Similarly, this improvement induced by **22h** could be dramatically decreased in HCT116 cells pretreated with 20 μM Z-VAD-FMK. Similarly, compound **1** still displayed weak caspase 3/7 activity in HCT116 cells pretreated with or without 20 μM Z-VAD-FMK. These preliminary data indicated that **22h** might mediate the apoptosis in HCT116 cells at low concentrations, at least partially, through activation of caspase 3/7.

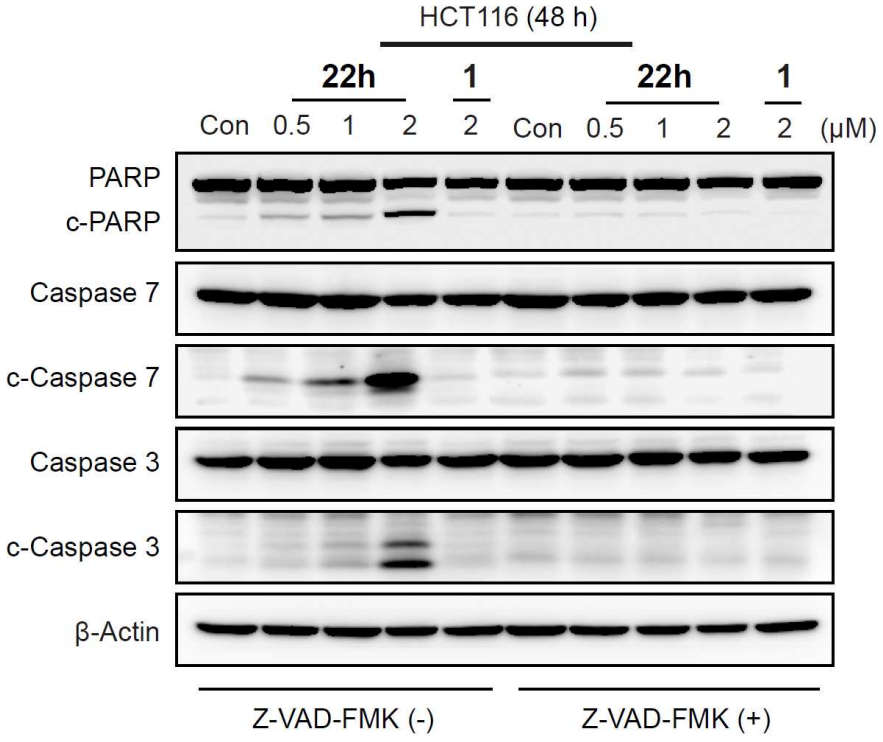

Figure 5. Compounds **22h** or **1** induced the cleavage of caspase 3/7 and PARP. HCT116 cells

pretreated with or without 20 μM Z-VAD-FMK for 1 h were exposed to **22h** or **1** for 48 h and analyzed by Western blotting.

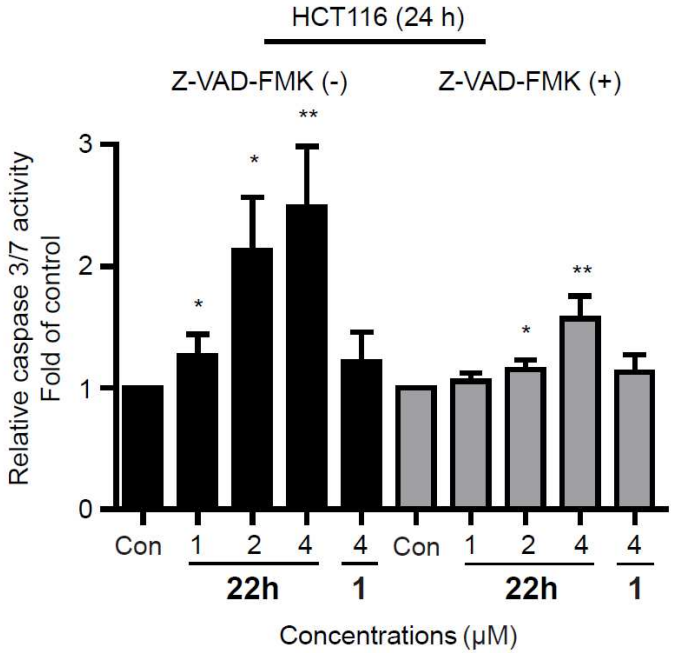

Figure 6. The changes in caspase 3/7 activity in HCT116 cells exposed to compound **22h** or **1** for 24 h were determined by Caspase-Glo® 3/7 assays. Data were expressed as mean ± SD from three independent experiments. Data were analyzed by Student *t* test. *, $p < 0.05$; **, $p < 0.01$.

Binding Interactions of Compound 22h with Human Kinases. To preliminary explore the possible interacting targets of **22h**, we performed the target screening of this compound against a panel of 468 kinases (including 403 non-mutated kinases) by using a competition binding assay at the DiscoveRx's KINOMEscan platform. As illustrated in Figure 7, compound **22h** did not show any significant binding interactions against almost all of tested kinases except CK2α and JAK3 with S(10) and S(35) selectivity scores of 0 and 0.005 at 1.0 μM, respectively (Tables S1 and S2). These results exclude the possibility that compound **22h** exerts its antitumor action through any of the well-known kinases as the target(s). Further mechanism studies of

22h on cell cycle and apoptosis are ongoing, and the results might be reported in due course.

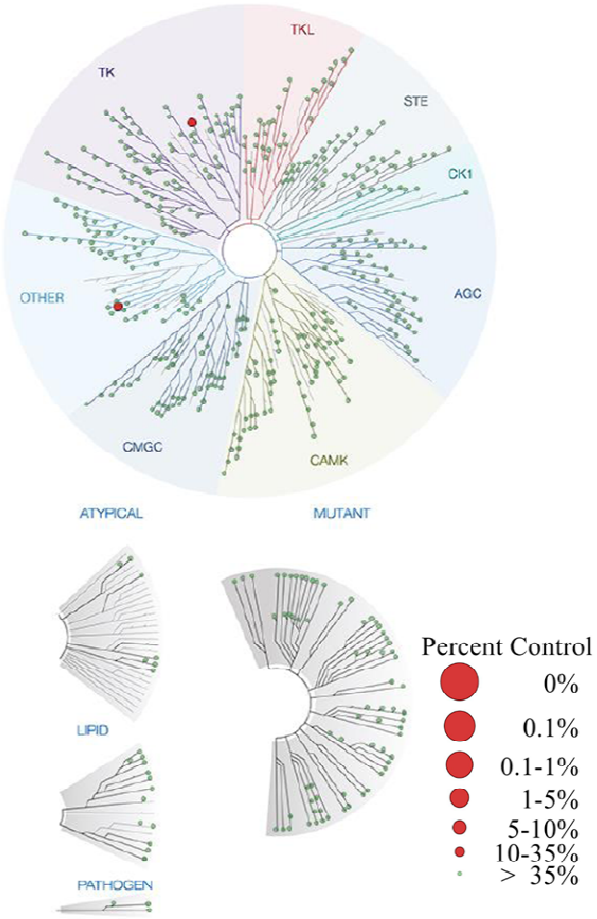

Figure 7. TREE*spot*™ Interaction Maps for compound **22h** against 468 kinases with DiscoveRx KINOMEscan profiling platform. Measurements were performed at a concentration of 1000 nM, and the affinity was defined as a percent of the DMSO control (% control), where the lower percentage represents stronger hits.

Compound 22h Suppressed the Growth of HCT116 Xenograft in Nude Mice. In our pilot *in vivo* studies, compound **22h** was further evaluated for its activity in suppression of tumor growth in the HCT116 xenograft model, and 5-FU was used as the positive control. As shown in Figure 8, mice treated with 30.0 mg/kg of **22h** *via* i.p. showed a significant effect in inhibiting tumor growth, while i.v. administration of

22h with 10.0 mg/kg displayed comparable potent inhibitory activity against tumor growth. Meanwhile, compound **22h** was found to be well tolerated during the experiments and showed no significant body weight loss.

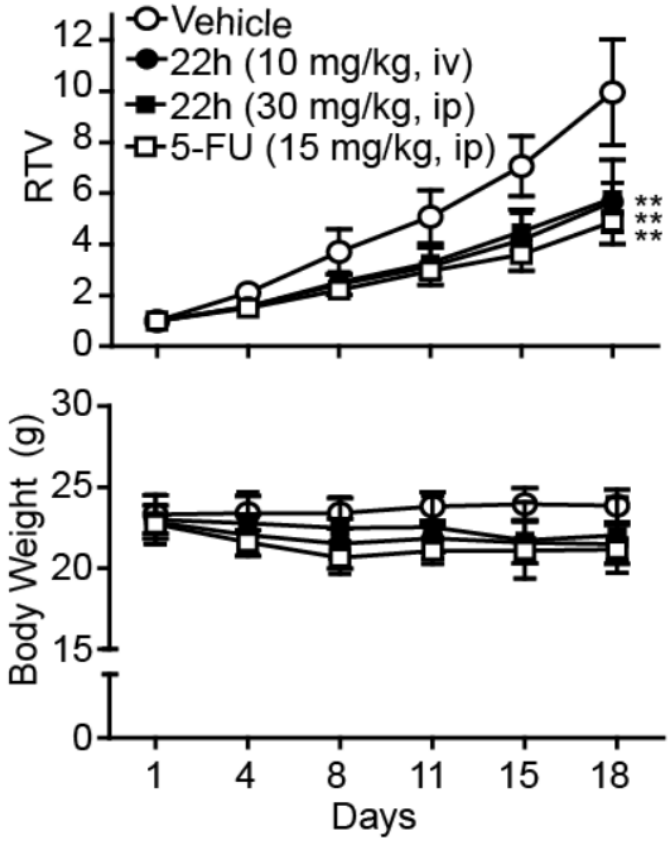

Figure 8. *In vivo* efficacy of compound **22h** in inhibiting growth of xenograft tumors (colon cancer HCT116) in mice at the doses of 10 mg/kg and 30 mg/kg (i.v. and i.p., respectively), 5-FU was used as positive controls. Upper: Relative tumor volume (RTV) changes; Lower: average body weight changes. Values are mean ± SD of 6 mice. Data were analyzed by Student *t* test. **, $P < 0.01$.

CONCLUSIONS

A broad and systemic structural modification on the natural product **1** was conducted with the aim to improve both the antitumor efficacy and the drug-like properties. Four

series of new tanshinone derivatives were synthesized and their antiproliferative effects against tumor cells were evaluated. It was found that incorporation of functional groups that help to increase aqueous solubility, such as amino or hydroxyl groups, to the B-ring or the furyl 17-methyl not only exhibited significantly enhanced antiproliferative activity against both KB and KB/VCR cells, but also displayed markedly improved aqueous solubility and metabolic stability relative to **1**. Particularly，the lactam derivative **22h** with *N*-3-(diethylamino)propyl side chain demonstrated the most potent antiproliferative activity with IC_{50} values of 0.12 and 0.33 μM, respectively, against KB and KB/VCR cells, which are approximately 13- to 49-fold more potent than **1**. This compound also showed a broad spectrum of antitumor potency against a panel of 9 human cancer cell lines. Meanwhile, **22h** possessed significantly improved drug-like properties including aqueous solubility (15.7 mg/mL), metabolic stability of liver microsomes, and PK characters ($T_{1/2}$ = 2.58 h; F = 21%). This compound significantly induced caspase 3/7-dependent apoptosis in HCT116 cells in a concentration-dependent manner, and likely mediated apoptosis. In nude mice bearing colon tumor xenografts, i.v. administration of **22h** at 10 mg/kg significantly suppressed the growth of HCT116 xenografts, and was found more efficacious than ip administration. Given the growing appreciation of natural products in drug discovery and the long historical use of the herb Danshen as a folk medicine, the markedly improved overall property of **22h** together with novel lactam scaffold deserves further investigating.

EXPERIMENTAL SECTION

Chemical Reagents and General Method. All commercially available starting materials and solvents are reagent grade, and used without further purification. Reactions were performed under a nitrogen atmosphere in dry glassware with magnetic stirring. Column chromatography was performed using 300−400 mesh silica gel purchased from Qingdao Haiyang Chemical Co.,Ltd. Analytical TLC was carried out employing silica gel 60 F254 plates (Merck, Darmstadt). Visualization of the developed chromatograms was performed with detection by UV (254 nm). NMR spectra were recorded on a Brucker-600 (^{1}H, 300 MHz; ^{13}C, 126 MHz) spectrometer with TMS as an internal reference. Chemical shifts downfield from TMS were expressed in ppm, and *J* values were given in Hz. High-resolution mass spectra (HRMS) were obtained from a Thermo Fisher LTQ Orbitrap Elite mass spectrometer. Parameters include the following: Nano ESI spray voltage was 1.8 kV; Capillary temperature was 275 ^{o}C and the resolution was 60,000; Ionization was achieved by positive mode. Melting points were measured on a Thermo Scientific Electrothermal Digital Melting Point Apparatus and uncorrected. Purity of final compounds was determined by analytical HPLC, which was carried out on a Shimadzu HPLC system (model: CBM-20A LC-20AD SPD-20A UV/VIS). HPLC analysis conditions: Waters μBondapak C18 (300 × 3.9 mm); flow rate 0.5 mL/min; UV detection at 270 and 254 nm; linear gradient from 30% acetonitrile in water (0.1% TFA) to 100% acetonitrile (0.1% TFA) in 20 min followed by 30 min of the last-named solvent. The purity of all biologically evaluated compounds is greater than 95%.

1-(Hydroxymethyl)-6-methylphenanthro[1,2-*b*]furan-10,11-dione (6)

To a solution of **1** (1.38 g, 5.0 mmol) in a mixture of 1,4-dioxane (20 mL) and H_2O (6 mL) was added SeO_2 (1.11 g, 10.0 mmol) under N_2 atmosphere. The resulting reaction mixture was stirred at 110 ºC for 72 h, and then poured into water and extracted with CH_2Cl_2 (30 mL × 3). The combined organic layer was washed with brine, dried over anhydrous Na_2SO_4, and concentrated *in vacuo* to give a dark red residue. The residue was further purified by silica gel column; elution with 25% EtOAc in hexane afforded the desired product **6** (380 mg, 26%) as a red solid. HPLC purity: 98.0%. ^{1}H NMR (300 MHz, $CDCl_3$): δ 9.26 (d, J = 8.9 Hz, 1H), 8.35 (d, J = 8.7 Hz, 1H), 7.85 (d, J = 8.7 Hz, 1H), 7.67 - 7.51 (m, 1H), 7.48 (s, 1H), 7.39 (d, J = 7.0 Hz, 1H), 4.71 (d, J = 7.7 Hz, 2H), 3.50 (t, J = 7.0 Hz, 1H), 2.71 (s, 3H). ^{13}C NMR (126 MHz, $CDCl_3$): δ 182.9, 176.0, 162.9, 141.4, 135.5, 134.3, 133.4, 133.0, 131.2, 129.2, 128.9, 126.6, 124.9, 123.4, 120.1, 118.9, 55.4, 20.0. MS (ESI, $[M + H]^+$) m/z 293.3.

1-(Bromomethyl)-6-methylphenanthro[1,2-*b*]furan-10,11-dione (7). To a solution of **6** (292 mg, 1.0 mmol) in anhydrous CH_2Cl_2 (10 mL) was added dropwise a solution of PBr_3 (325 mg, 1.2 mmol) in CH_2Cl_2 (2 mL) at 0 ºC. The resulting reaction mixture was stirred at rt for 3 h, and then quenched by saturated $NaHCO_3$ aqueous solution and extracted with CH_2Cl_2 (30 mL × 3). The combined organic layer was washed with brine, dried over anhydrous Na_2SO_4, and concentrated *in vacuo* to give a dark red residue. The residue was further purified by silica gel column; elution with 10% EtOAc in hexane afforded the desired product **7** (255 mg, 72%) as a red solid. ^{1}H NMR (300 MHz, $CDCl_3$): δ 9.28 (d, J = 8.7 Hz, 1H), 8.36 (d, J = 8.6 Hz, 1H), 7.85 (d,

J = 8.6 Hz, 1H), 7.65 - 7.52 (m, 2H), 7.39 (d, *J* = 6.9 Hz, 1H), 4.59 (s, 2H), 2.71 (s, 3H). ^{13}C NMR (126 MHz, $CDCl_3$): δ 182.7, 174.8, 162.0, 144.3, 135.5, 134.1, 133.3, 132.9, 131.1, 129.1, 128.8, 124.9, 123.8, 123.5, 118.8, 118.6, 20.4, 20.0.

General Experimental Procedure for Synthesis of Compounds 8a-r:

A mixture of **7** (18 mg, 0.05 mmol), various amines (0.15 mmol) and K_2CO_3 (21 mg, 0.15 mmol) in THF (0.4 mL) and CH_3CN (1.2 mL) was stirred at rt until **7** was completely consumed as indicated by TLC. The reaction mixture was diluted with water and extracted with CH_2Cl_2 (30 mL × 3). The combined organic layer was washed with brine, dried over anhydrous Na_2SO_4, and concentrated *in vacuo* to give a dark red residue. The residue was further purified by silica gel column; elution with 2-5% MeOH in CH_2Cl_2 afforded the desired product **8a-r** as red solids in 46-95% yields.

1-((Dimethylamino)methyl)-6-methylphenanthro[1,2-*b*]furan-10,11-dione (8a). Yield: 59%. Mp: 215−216 °C. HPLC purity: 97.5%. ^{1}H NMR (300 MHz, $CDCl_3$): δ 9.23 (d, *J* = 8.9 Hz, 1H), 8.29 (d, *J* = 8.7 Hz, 1H), 7.80 (d, *J* = 8.7 Hz, 1H), 7.58 - 7.48 (m, 2H), 7.34 (d, *J* = 7.0 Hz, 1H), 3.67 (s, 2H), 2.68 (s, 3H), 2.37 (s, 7H). ^{13}C NMR (126 MHz, $CDCl_3$): δ 183.2, 175.4, 161.5, 143.7, 135.4, 133.8, 133.1, 132.8, 130.9, 129.6, 128.6, 124.9, 123.4, 123.2, 119.9, 118.8, 52.3, 45.4 (2), 20.0. MS (ESI, $[M + H]^+$) m/z 320.3. HRMS (ESI) calcd for $C_{20}H_{18}NO_3$, 320.1281; found, 320.1275.

1-((Methoxy(methyl)amino)methyl)-6-methylphenanthro[1,2-*b*]furan-10,11-dione (8b). Yield: 67%. Mp: 216−218 °C. HPLC purity: 98.3%. ^{1}H NMR (300 MHz, $CDCl_3$): δ 9.23 (d, *J* = 8.9 Hz, 1H), 8.29 (d, *J* = 8.7 Hz, 1H), 7.81 (d, *J* = 8.7 Hz, 1H),

7.59 - 7.47 (m, 2H), 7.34 (d, J = 6.9 Hz, 1H), 4.00 (s, 2H), 3.54 (s, 3H), 2.68 (s, 6H). ^{13}C NMR (126 MHz, $CDCl_3$): δ 183.2, 175.4, 161.3, 144.0, 135.4, 133.8, 133.1, 132.9, 130.9, 129.6, 128.6, 124.9, 123.2, 122.2, 119.9, 118.9, 59.9, 52.7, 44.6, 20.0. MS (ESI, $[M + H]^+$) m/z 336.3. HRMS (ESI) calcd for $C_{20}H_{18}NO_4$, 336.1230; found, 336.1227.

1-(((2-Hydroxyethyl)(methyl)amino)methyl)-6-methylphenanthro[1,2-*b*]furan-10, 11-dione (8c). Yield: 87%. Mp: 213−214 °C. HPLC purity: 97.7%. ^{1}H NMR (300 MHz, $CDCl_3$): δ 9.24 (d, J = 8.9 Hz, 1H), 8.32 (d, J = 8.7 Hz, 1H), 7.83 (d, J = 8.7 Hz, 1H), 7.60 - 7.52 (m, 1H), 7.50 (s, 1H), 7.36 (d, J = 6.9 Hz, 1H), 3.76 - 3.68 (m, 4H), 2.73 - 2.65 (m, 5H), 2.33 (s, 3H). ^{13}C NMR (126 MHz, $CDCl_3$): δ 183.2, 175.4, 162.2, 143.6, 135.4, 134.0, 133.2, 132.9, 130.9, 129.5, 128.7, 125.0, 123.7, 123.4, 119.9, 118.9, 59.0, 58.9, 50.4, 42.2, 20.0. MS (ESI, $[M + H]^+$) m/z 350.3. HRMS (ESI) calcd for $C_{21}H_{20}NO_4$, 350.1387; found, 350.1381.

1-((Bis(2-hydroxyethyl)amino)methyl)-6-methylphenanthro[1,2-*b*]furan-10,11-di one (8d). Yield: 58%. Mp: 211−212 °C. HPLC purity: 98.8%. ^{1}H NMR (300 MHz, $CDCl_3$) δ 9.19 (d, J = 8.9 Hz, 1H), 8.26 (d, J = 8.7 Hz, 1H), 7.77 (d, J = 8.8 Hz, 1H), 7.62 - 7.47 (m, 2H), 7.34 (d, J = 7.0 Hz, 1H), 3.81 - 3.65 (m, 6H), 2.74 - 2.66 (m, 4H), 2.65 (s, 3H). ^{13}C NMR (126 MHz, $CDCl_3$): δ 182.8, 175.5, 163.2, 144.0, 135.4, 134.0, 133.2, 132.8, 131.1, 129.3, 128.8, 124.9, 124.0, 123.3, 119.7, 118.9, 59.4 (2), 55.8 (2), 47.8, 20.0. MS (ESI, $[M + H]^+$) m/z 380.3. HRMS (ESI) calcd for $C_{22}H_{22}NO_5$, 380.1492; found, 380.1490.

1-((Bis(2-chloroethyl)amino)methyl)-6-methylphenanthro[1,2-*b*]furan-10,11-dion e (8e). Yield: 46%. Mp: 214−215 °C. HPLC purity: 98.2%. ^{1}H NMR (300 MHz,

$CDCl_3$): δ 9.26 (d, J = 8.9 Hz, 1H), 8.35 (d, J = 8.7 Hz, 1H), 7.86 (d, J = 8.7 Hz, 1H), 7.65 - 7.51 (m, 2H), 7.38 (d, J = 6.6 Hz, 1H), 3.93 (s, 2H), 3.61 (t, J = 6.8 Hz, 4H), 2.99 (t, J = 6.8 Hz, 4H), 2.71 (s, 3H). ^{13}C NMR (126 MHz, $CDCl_3$) δ 183.19, 175.36, 161.91, 143.61, 135.29, 133.89, 133.15, 132.83, 130.86, 129.48, 128.57, 124.81, 124.32, 123.28, 119.52, 118.76, 56.40, 48.45, 42.09, 19.89. MS (ESI, $[M + H]^+$) m/z 416.3. HRMS (ESI) calcd for $C_{22}H_{20}Cl_2NO_3$, 416.0815; found, 416.0808.

6-Methyl-1-(morpholinomethyl)phenanthro[1,2-*b*]furan-10,11-dione (8f). Yield: 88%. Mp: 212−213 °C. HPLC purity: 97.8%. ^{1}H NMR (300 MHz, $CDCl_3$): δ 9.21 (d, J = 8.7 Hz, 1H), 8.27 (d, J = 8.6 Hz, 1H), 7.78 (d, J = 8.6 Hz, 1H), 7.56 - 7.49 (m, 1H), 7.47 (s, 1H), 7.33 (d, J = 6.6 Hz, 1H), 3.80 - 3.65 (m, 4H), 2.67 (s, 3H), 2.53 - 2.63 (m, 4H). ^{13}C NMR (126 MHz, $CDCl_3$): δ 183.3, 175.4, 161.7, 143.6, 135.4, 133.9, 133.2, 132.9, 130.9, 129.6, 128.6, 124.9, 123.3, 122.8, 120.0, 118.8, 67.1 (2), 53.5 (2), 51.6, 20.0. MS (ESI, $[M + H]^+$) m/z 362.1. HRMS (ESI) calcd for $C_{22}H_{20}NO_4$, 362.1387; found, 362.1384.

(*S*)-1-((2-(Hydroxymethyl)morpholino)methyl)-6-methylphenanthro[1,2-*b*]furan-10,11-dione (8g). Yield: 61%. Mp: 210−211 °C. HPLC purity: 96.5%. ^{1}H NMR (300 MHz, $CDCl_3$): δ ^{1}H NMR (300 MHz, $CDCl_3$) δ 9.26 (d, J = 8.9 Hz, 1H), 8.34 (dd, J = 8.7, 0.9 Hz, 1H), 7.85 (d, J = 8.8 Hz, 1H), 7.57 (dd, J = 8.9, 7.0 Hz, 1H), 7.48 (d, J = 1.1 Hz, 1H), 7.37 (d, J = 7.0 Hz, 1H), 3.95 – 3.90 (m, 1H), 3.78 – 3.55 (m, 6H), 2.86 – 2.80 (m, 2H), 2.71 (s, 3H), 2.34 (td, J = 11.3, 3.4 Hz, 1H), 2.15 (dd, J = 11.2, 9.9 Hz, 1H), 1.96 (s, 1H). ^{13}C NMR (126 MHz, $CDCl_3$) δ 183.22, 175.34, 161.65, 143.49, 135.26, 133.84, 133.10, 132.83, 130.83, 129.50, 128.55, 124.82, 123.30, 122.54,

119.93, 118.73, 75.97, 66.64, 64.24, 54.30, 52.79, 51.31, 19.89. MS (ESI, $[M + H]^+$) m/z 392.4. HRMS (ESI) calcd for $C_{23}H_{22}NO_5$, 392.1492; found, 392.1480.

6-Methyl-1-((4-oxopiperidin-1-yl)methyl)phenanthro[1,2-*b*]furan-10,11-dione (8h). Yield: 78%. Mp: 213−214 °C. HPLC purity: 97.9%. ^{1}H NMR (300 MHz, $CDCl_3$): δ 9.24 (d, J = 8.9 Hz, 1H), 8.31 (d, J = 8.7 Hz, 1H), 7.82 (d, J = 8.7 Hz, 1H), 7.59 - 7.49 (m, 2H), 7.36 (d, J = 7.0 Hz, 1H), 3.85 (s, 2H), 2.91 (t, J = 6.1 Hz, 4H), 2.69 (s, 3H), 2.49 (t, J = 6.0 Hz, 4H). ^{13}C NMR (126 MHz, $CDCl_3$): δ 208.9, 183.1, 175.4, 161.8, 143.5, 135.4, 133.9, 133.2, 132.9, 130.9, 129.5, 128.7, 124.9, 123.3, 123.2, 119.9, 118.8, 52.9 (2), 50.4, 41.39 (2), 20.0. MS (ESI, $[M + H]^+$) m/z 374.2. HRMS (ESI) calcd for $C_{23}H_{20}NO_4$, 374.1387; found, 374.1374.

1-((4-Hydroxypiperidin-1-yl)methyl)-6-methylphenanthro[1,2-*b*]furan-10,11-dione (8i). Yield: 88%. Mp: 210−211 °C. HPLC purity: 98.6%. ^{1}H NMR (300 MHz, $CDCl_3$): δ 9.24 (d, J = 8.9 Hz, 1H), 8.31 (d, J = 8.7 Hz, 1H), 7.82 (d, J = 8.7 Hz, 1H), 7.60 - 7.52 (m, 1H), 7.51 (s, 1H), 7.35 (d, J = 6.9 Hz, 1H), 3.80 - 3.70 (m, 3H), 2.99 - 2 .86 (m, 2H), 2.69 (s, 3H), 2.28 - 2.42 (m, 2H), 2.0 - 1.87 (m, 2H), 1.71 - 1.55 (m, 2H). ^{13}C NMR (126 MHz, $CDCl_3$): δ 183.3, 175.5, 161.6, 143.8, 135.4, 133.9, 133.2, 132.9, 130.9, 129.7, 128.6, 124.9, 123.3, 120.1, 118.9, 67.7, 51.1 (2), 50.9 (2), 34.6, 20.0. MS (ESI, $[M + H]^+$) m/z 376.4. HRMS (ESI) calcd for $C_{23}H_{22}NO_4$, 376.1543; found, 376.1535.

1-((4-(Dimethylamino)piperidin-1-yl)methyl)-6-methylphenanthro[1,2-*b*]furan-10,11-dione (8j). Yield: 64%. Mp: 213−214 °C. HPLC purity: 97.0%. ^{1}H NMR (300 MHz, $CDCl_3$): δ 9.28 (d, J = 8.9 Hz, 1H), 8.36 (d, J = 8.6 Hz, 1H), 7.88 (d, J = 8.7 Hz,

1H), 7.61 – 7.56 (m, 1H), 7.51 (s, 1H), 7.38 (d, J = 7.0 Hz, 1H), 3.74 (s, 2H), 3.13 (d, J = 11.3 Hz, 2H), 2.72 (s, 3H), 2.50 – 2.43 (m, 7H), 2.18 (t, J = 11.7 Hz, 2H), 1.99 – 1.95 (m, 2H), 1.70 – 1.67 (m, 2H). ^{13}C NMR (126 MHz, $CDCl_3$) δ 183.16, 175.39, 161.70, 143.96, 135.34, 133.84, 133.26, 132.78, 130.84, 129.52, 128.53, 124.64, 123.08, 122.21, 119.81, 118.76, 62.45, 52.06, 50.42, 40.50, 26.93, 19.77. MS (ESI, $[M + H]^+$) m/z 403.5. HRMS (ESI) calcd for $C_{25}H_{27}N_2O_3$, 403.2016; found, 403.2020.

6-Methyl-1-((4-methylpiperazin-1-yl)methyl)phenanthro[1,2-*b*]furan-10,11-dione (8k). Yield: 95%. Mp: 209−210 °C. HPLC purity: 99.0%. ^{1}H NMR (300 MHz, $CDCl_3$): δ 9.26 (d, J = 8.9 Hz, 1H), 8.33 (d, J = 8.7 Hz, 1H), 7.84 (d, J = 8.7 Hz, 1H), 7.56 (dd, J = 8.9, 6.9 Hz, 1H), 7.47 (s, 1H), 7.36 (d, J = 6.9 Hz, 1H), 3.76 (s, 3H), 2.70 (s, 3H), 2.65 (brs, 4H), 2.49 (brs, 4H), 2.30 (s, 3H). ^{13}C NMR (126 MHz, $CDCl_3$) δ 183.24, 175.33, 161.44, 143.43, 135.23, 133.76, 133.03, 132.79, 130.75, 129.54, 128.46, 124.80, 123.18, 122.85, 120.01, 118.72, 55.10, 52.72, 50.99, 45.99, 19.88. MS (ESI, $[M + H]^+$) m/z 375.3. HRMS (ESI) calcd for $C_{23}H_{23}N_2O_3$, 375.1703; found, 375.1705.

1-((4-(2-Hydroxyethyl)piperazin-1-yl)methyl)-6-methylphenanthro[1,2-*b*]furan-10,11-dione (8l). Yield: 53%. Mp: 215−217 °C. HPLC purity: 96.2%. ^{1}H NMR (300 MHz, $CDCl_3$): δ 9.25 (d, J = 8.9 Hz, 1H), 8.32 (d, J = 8.8 Hz, 1H), 7.84 (d, J = 8.7 Hz, 1H), 7.56 (dd, J = 8.9, 7.0 Hz, 1H), 7.47 (s, 1H), 7.36 (d, J = 7.0 Hz, 1H), 3.75 (d, J = 1.1 Hz, 2H), 3.60 (t, J = 5.4 Hz, 2H), 2.70 – 2.53 (m, 13H), 2.05 (s, 1H). ^{13}C NMR (126 MHz, $CDCl_3$) δ 183.23, 175.35, 161.49, 143.45, 135.24, 133.77, 133.04, 132.79, 130.77, 129.54, 128.49, 124.81, 123.22, 122.81, 120.00, 118.73, 59.16, 57.73, 52.83,

50.95, 19.88. MS (ESI, $[M + H]^+$) m/z 405.3. HRMS (ESI) calcd for $C_{24}H_{25}N_2O_4$, 405.1809; found, 405.1807.

6-Methyl-1-(pyrrolidin-1-ylmethyl)phenanthro[1,2-*b*]furan-10,11-dione (8m). Yield: 82%. Mp: 210−211 °C. HPLC purity: 97.6%. ^{1}H NMR (300 MHz, $CDCl_3$): δ 9.24 (d, J = 8.9 Hz, 1H), 8.32 (d, J = 8.7 Hz, 1H), 7.83 (d, J = 8.7 Hz, 1H), 7.63 (s, 1H), 7.55 (dd, J = 8.8, 7.0 Hz, 1H), 7.36 (d, J = 7.0 Hz, 1H), 3.93 (s, 2H), 2.79 – 2.75 (m, 4H), 2.69 (s, 3H), 1.89 – 1.85 (m, 4H); ^{13}C NMR (126 MHz, $CDCl_3$) δ 183.15, 175.44, 161.36, 144.11, 135.27, 133.80, 133.08, 132.78, 130.79, 129.49, 128.50, 124.77, 123.16, 119.54, 118.78, 54.02, 48.54, 23.57, 19.88. MS (ESI, $[M + H]^+$) m/z 346.3. HRMS (ESI) calcd for $C_{22}H_{20}NO_3$, 346.1438; found, 346.1437.

1-((3-(Hydroxymethyl)pyrrolidin-1-yl)methyl)-6-methylphenanthro[1,2-*b*]furan-10,11-dione (8n). Yield: 78%. Mp: 211−212 °C. HPLC purity: 97.4%. ^{1}H NMR (300 MHz, $CDCl_3$): δ 9.25 (d, J = 8.9 Hz, 1H), 8.33 (d, J = 8.7 Hz, 1H), 7.85 (d, J = 8.7 Hz, 1H), 7.62 – 7.51 (m, 2H), 7.37 (d, J = 7.0 Hz, 1H), 3.85 (s, 2H), 3.71 (dd, J = 10.1, 4.4 Hz, 1H), 3.56 (dd, J = 10.1, 5.1 Hz, 1H), 3.03 – 2.95 (m, 1H), 2.84 (dd, J = 9.3, 3.5 Hz, 1H), 2.75 – 2.67 (m, 4H), 2.54 (q, J = 8.5 Hz, 1H), 2.44 – 2.37 (m, 1H), 2.11 – 2.01 (m, 2H), 1.79 – 1.71 (m, 1H). ^{13}C NMR (126 MHz, $CDCl_3$) δ 183.18, 175.38, 161.49, 143.58, 135.26, 133.83, 133.08, 132.80, 130.79, 129.49, 128.51, 124.80, 123.50, 123.24, 119.56, 118.77, 67.19, 57.90, 53.78, 48.27, 38.92, 26.99, 19.88. MS (ESI, $[M + H]^+$) m/z 346.3. HRMS (ESI) calcd for $C_{23}H_{22}NO_4$, 376.1543; found, 376.1542.

(*S*)-1-((3-(Dimethylamino)pyrrolidin-1-yl)methyl)-6-methylphenanthro[1,2-*b*]fur

an-10,11-dione (8o). Yield: 55%. Mp: 212−213 °C. HPLC purity: 95.8%. ^{1}H NMR (300 MHz, $CDCl_3$): δ 9.20 (d, J = 8.8 Hz, 1H), 8.29 (d, J = 8.7 Hz, 1H), 7.79 (d, J = 8.7 Hz, 1H), 7.60 - 7.46 (m, 2H), 7.33 (d, J = 6.9 Hz, 1H), 3.82 (s, 2H), 3.45 - 3.35 (m, 1H), 3.14 - 2.76 (m, 4H), 2.67 (s, 3H), 2.53 (s, 6H), 2.35 - 1.85 (m, 2H). ^{13}C NMR (126 MHz, $CDCl_3$) δ 183.25, 175.35, 161.51, 143.46, 135.26, 133.81, 133.08, 132.80, 130.78, 129.54, 128.50, 124.78, 123.48, 123.23, 119.64, 118.77, 65.23, 57.57, 53.01, 48.42, 43.13, 28.42, 19.88. MS (ESI, $[M + H]^+$) m/z 389.2. HRMS (ESI) calcd for $C_{24}H_{25}N_2O_3$, 389.1860; found, 389.1857.

3-Hydroxy-8-methyl-2-(2-methylprop-1-en-1-yl)phenanthrene-1,4-dione (10). To a solution of **9** (95 mg, 0.4 mmol) in dry toluene (20 mL) was added methylamine hydrochloride (40 mg, 0.6 mmol), isobutyraldehyde (182 μL, 2.0 mmol) and *p*-toluenesulfonic acid (95 mg, 0.5 mmol). The reaction mixture was then refluxed in a system equipped with a DeaneStark trap for 3 h. The reaction mixture was then concentrated in vacuo, and the crude residue was further purified by silica gel column; elution with 10% EtOAc in hexane afforded the desired product **10** as yellow solid. Yield: 94%. Mp: 220−222 °C. ^{1}H NMR (300 MHz, $CDCl_3$): δ 9.44 (d, J = 8.8 Hz, 1H), 8.39 (d, J = 8.8 Hz, 1H), 8.25 (d, J = 8.8 Hz, 1H), 7.93 (s, 1H), 7.62 (t, J = 7.9 Hz, 1H), 7.46 (d, J = 6.9 Hz, 1H), 6.02 (s, 1H), 2.73 (s, 3H), 2.00 (s, 3H), 1.71 (s, 3H).

2,2,6-Trimethyl-1,2-dihydrophenanthro[1,2-*b*]furan-10,11-dione (11). To a solution of **9** (29 mg, 0.1 mmol) in anhydrous CH_2Cl_2 (4 mL) was added anhydrous $AlCl_3$ (53 mg, 0.4 mmol) under N_2 atmosphere. The resulting mixture was stirred at rt for 6 h, then quenched by H_2O and extracted with CH_2Cl_2 (30 mL × 3). The combined

organic layer was washed with brine, dried over anhydrous Na_2SO_4, and concentrated *in vacuo* to give a dark red residue. The residue was further purified by silica gel column; elution with 20% EtOAc in hexane afforded the desired product **11** as red solid in 72% yield. Mp: 182−184 °C. HPLC purity: 98.8%. ^{1}H NMR (300 MHz, $CDCl_3$): δ 9.32 (d, J = 9.0 Hz, 1H), 8.32 (d, J = 8.7 Hz, 1H), 7.79 (d, J = 8.7 Hz, 1H), 7.66 – 7.53 (m, 1H), 7.41 (d, J = 6.5 Hz, 1H), 2.97 (s, 2H), 2.72 (s, 3H), 1.64 (s, 6H). ^{13}C NMR (126 MHz, $CDCl_3$) δ 184.41, 176.03, 169.43, 134.94, 134.85, 132.18, 131.80, 130.39, 128.82, 128.70, 126.35, 125.13, 120.48, 113.27, 93.55, 39.26, 28.47(2C), 19.89. MS (ESI, $[M + H]^+$) m/z 293.3. HRMS (ESI) calcd for $C_{19}H_{17}O_3$, 293.1172; found, 293.1170.

1-Hydroxy-2,2,6-trimethyl-1,2-dihydrophenanthro[1,2-*b*]furan-10,11-dione (12). To a solution of **9** (29 mg, 0.1 mmol) in anhydrous CH_2Cl_2 (2 mL) was added Br_2 (53 mg, 0.2 mmol) under N_2 atmosphere. The resulting mixture was stirred at rt for 6 h, and then evaporated *in vacuo* to give the bromo intermediate as a red residue. To a solution of the residue in CH_2Cl_2 (2 mL) was added saturated $NaHSO_3$ aqueous solution (1 mL). The resulting mixture was stirred at rt for 30 min, and then saturated Na_2CO_3 aqueous solution was added to make the PH value greater than 9. After stirring at rt for three days, the reaction solution was extracted with CH_2Cl_2 (30 mL×3). The combined organic layer was washed with brine, dried over anhydrous Na_2SO_4, and concentrated *in vacuo* to give a dark red residue. The residue was further purified by silica gel column; elution with 20% EtOAc in hexane afforded the desired product **12** as red solid in 63% yield. Mp: 188−189 °C. HPLC purity: 98.2%. ^{1}H

NMR (300 MHz, DMSO): δ 9.16 (d, J = 8.9 Hz, 1H), 8.48 (d, J = 8.5 Hz, 1H), 7.81 (d, J = 8.6 Hz, 1H), 7.65 (dd, J = 8.9, 6.9 Hz, 1H), 7.52 (d, J = 6.9 Hz, 1H), 5.55 (d, J = 7.4 Hz, 1H), 4.70 (d, J = 7.4 Hz, 1H), 2.70 (s, 3H), 1.55 (s, 3H), 1.44 (s, 3H). ^{13}C NMR (126 MHz, DMSO): δ 184.0, 175.2, 169.1, 135.4, 134.3, 132.4, 131.3, 130.3, 128.8, 128.1, 126.4, 124.3, 120.5, 116.2, 96.1, 74.4, 26.0, 20.7, 19.5. MS (ESI, $[M + H]^+$) m/z 309.3. HRMS (ESI) calcd for $C_{19}H_{17}O_4$, 309.1121; found, 309.1119.

1-Methoxy-2,2,6-trimethyl-1,2-dihydrophenanthro[1,2-*b*]furan-10,11-dione (13). To a solution of **9** (29 mg, 0.1 mmol) in anhydrous CH_2Cl_2 (2 mL) was added Br_2 (53 mg, 0.2 mmol) under N_2 atmosphere. The resulting reaction mixture was stirred at rt for 6 h, and then anhydrous MeOH was added into it. After stirring for 3 h, the resulting reaction mixture was concentrated *in vacuo* to give a dark red residue. The residue was further purified by silica gel column; elution with 20% EtOAc in hexane afforded the desired product **13** as red solid in 40% yield. Mp: 190−192 °C. HPLC purity: 96.5%. ^{1}H NMR (300 MHz, $CDCl_3$): δ 9.33 (d, J = 9.0 Hz, 1H), 8.33 (d, J = 8.7, 1H), 7.83 (d, J = 8.7 Hz, 1H), 7.64 - 7.55 (m, 1H), 7.43 (d, J = 7.1 Hz, 1H), 4.50 (s, 1H), 3.57 (s, 3H), 2.72 (s, 3H), 1.67 (s, 3H), 1.51 (s, 3H). ^{13}C NMR (126 MHz, $CDCl_3$): δ 184.3, 176.4, 171.9, 135.3, 135.1, 132.2, 132.1, 130.6, 129.3, 128.4, 127.1, 125.4, 120.7, 115.1, 95.9, 84.0, 59.2, 27.0, 20.8, 20.1. MS (ESI, $[M + H]^+$) m/z 323.2. HRMS (ESI) calcd for $C_{20}H_{19}O_4$, 323.1278; found, 323.1278.

General Experimental Procedure for Synthesis of Compounds 14a-b:

To a solution of **9** (29 mg, 0.1 mmol) in anhydrous CH_2Cl_2 (2 mL) was added Br_2 (53 mg, 0.2 mmol) under N_2 atmosphere. The resulting mixture was stirred at rt for 6 h,

and then evaporated *in vacuo* to give the bromo intermediate as red residue. To a solution of the residue in CH_2Cl_2 (2 mL) was added an excess of the appropriate arylamine. The resulting reaction mixture was stirred overnight, after which the crude product was poured into 50 mL of water. The organic phase was separated and washed with 10% HCl (3×50 mL), dried over sodium sulfate, filtered, and evaporated under reduced pressure to yield a solid, which was purified by column chromatography in silica gel; elution with 20-40% EtOAc in hexane afforded the desired products **14a-b** as red solids.

1-((2,5-Dimethoxyphenyl)amino)-2,2,6-trimethyl-1,2-dihydrophenanthro[1,2-*b*]furan-10,11-dione (14a). Yield: 59%. Mp: 192−193 °C. HPLC purity: 97.0%. ^{1}H NMR (300 MHz, $CDCl_3$): δ 9.32 (d, J = 8.9 Hz, 1H), 8.35 (d, J = 8.7 Hz, 1H), 7.84 (d, J = 8.7 Hz, 1H), 7.65 - 7.53 (m, 1H), 7.44 (d, J = 6.9 Hz, 1H), 6.67 (d, J = 8.4 Hz, 1H), 6.18 (d, J = 8.4 Hz, 2H), 6.17 (s, 1H), 4.78 (d, J = 6.7 Hz, 1H), 4.55 (d, J = 6.7 Hz, 1H), 3.76 (s, 6H), 2.73 (s, 3H), 1.70 (s, 3H), 1.61 (s, 3H). ^{13}C NMR (126 MHz, $CDCl_3$): δ 184.2, 175.7, 170.4, 154.7, 141.7, 138.5, 135.2, 135.2, 132.3, 132.1, 130.7, 129.3, 128.3, 127.0, 125.3, 120.7, 113.7, 110.6, 99.4, 98.8, 96.8, 61.4, 56.4, 55.7, 27.6, 21.69, 20.1. MS (ESI, $[M + H]^+$) m/z 444.3. HRMS (ESI) calcd for $C_{27}H_{26}NO_5$, 444.1805; found, 444.1815.

1-((4-Fluoro-3-nitrophenyl)amino)-2,2,6-trimethyl-1,2-dihydrophenanthro[1,2-*b*]furan-10,11-dione (14b). Yield: 60%. Mp: 191−192 °C. HPLC purity: 97.5%. ^{1}H NMR (300 MHz, DMSO): δ 9.19 (d, J = 8.9 Hz, 1H), 8.51 (d, J = 8.7 Hz, 1H), 7.86 (d, J = 8.7 Hz, 1H), 7.68 (dd, J = 8.9, 6.9 Hz, 1H), 7.54 (d, J = 6.9 Hz, 1H), 7.38 - 7.23

(m, 2H), 7.06 (dt, *J* = 9.1, 3.4 Hz, 1H), 6.59 (d, *J* = 8.6 Hz, 1H), 4.85 (d, *J* = 8.6 Hz, 1H), 2.71 (s, 3H), 1.66 (s, 3H), 1.50 (s, 3H). ^{13}C NMR (126 MHz, DMSO) δ 184.16, 175.40, 169.07, 146.55 (d, *J* = 275.9 Hz), 145.41 (d, *J* = 32.7 Hz), 137.67 (d, *J* = 8.8 Hz), 135.98, 134.86, 132.98, 131.83, 130.90, 129.33, 128.48, 126.80, 124.66, 120.91, 119.42, 119.35 (d, *J* = 31.5 Hz), 114.43 (d, *J* = 3.8 Hz), 107.58, 96.19, 60.40, 27.33, 21.83, 19.91. MS (ESI, $[M + Na]^+$) m/z 469.3. HRMS (ESI) calcd for $C_{25}H_{19}FN_2NaO_5$, 469.1170; found, 469.1179.

1,2,6-Trimethoxy-4-(prop-2-yn-1-yloxy)phenanthridine (17). A mixture of **16** (285 mg, 1.0 mmol), 3-bromoprop-1-yne (595 mg, 5.0 mmol) and K_2CO_3 (276 mg, 2.0 mmol) in acetone (5 mL) was stirred at 60 ^{o}C for 8 h. The reaction mixture was concentrated in vaccuo to provide the crude residue. The residue was diluted with CH_2Cl_2 (20 mL), and then washed with brine, dried over anhydrous Na_2SO_4, and concentrated *in vacuo* to give a brown residue which was further purified by silica gel column with 20% EtOAc in hexane to afford the desired product **17** as a colorless solid in 98% yield. ^{1}H NMR (300 MHz, $CDCl_3$) δ 9.38 (d, *J* = 8.6 Hz, 1H), 8.31 (d, *J* = 8.0 Hz, 1H), 7.74 (t, *J* = 8.5, 7.1 Hz, 1H), 7.58 (t, *J* = 7.5 Hz, 1H), 7.11 (s, 1H), 5.05 (d, *J* = 2.2 Hz, 2H), 4.17 (s, 3H), 3.94 (s, 3H), 3.87 (s, 3H), 2.48 (t, *J* = 2.2 Hz, 1H). MS (ESI, $[M + H]^+$) m/z 324.3.

5,10,11-Trimethoxy-2-methylfuro[3,2-*c*]phenanthridine (18). To a solution of **17** (323 mg, 1.0 mmol**)** in *N*,*N*-diethylaniline (5 mL) was added CsF (608 mg, 4.0 mmol). The resulting mixture stirred at 200 ^{o}C for 8 h, and then CH_2Cl_2 (20 mL) and 1N HCl aqueous solution were added to make the PH value less than 5. The resulting mixture

was washed with brine, dried over anhydrous Na_2SO_4, and concentrated *in vacuo* to give a brown residue. The residue was further purified by silica gel column; elution with 20% EtOAc in hexane afforded the desired product **18** in 69% yield as a colorless solid. ^{1}H NMR (300 MHz, $CDCl_3$) δ 9.44 (d, J = 8.6 Hz, 1H), 8.43 (d, J = 8.1 Hz, 1H), 7.81 (t, J = 7.9 Hz, 1H), 7.62 (t, J = 7.4 Hz, 1H), 6.65 (s, 1H), 4.33 (s, 3H), 4.14 (s, 3H), 3.98 (s, 3H), 2.61 (s, 3H). MS (ESI, $[M + H]^+$) m/z 324.5.

10,11-Dimethoxy-2-methylfuro[3,2-*c*]phenanthridin-5(4*H*)-one (19). To a solution of **18** (323 mg, 1.0 mmol) and NaI (300 mg, 2.0 mmol) in anhydrous CH_2Cl_2 (15 mL) was added TMSI dropwise at rt. The resulting mixture was stirred at rt for 4 h, and then quenched by 5% $Na_2S_2O_3$ aqueous solution. The resulting mixture was washed with brine, dried over anhydrous Na_2SO_4, and concentrated *in vacuo* to give a brown residue. The residue was further purified by silica gel column; elution with 20% EtOAc in hexane afforded the desired product **19** as a colorless solid in 98% yield. ^{1}H NMR (300 MHz, $CDCl_3$) δ 9.43 (s, 1H), 9.21 (d, J = 8.5 Hz, 1H), 8.60 (d, J = 7.9 Hz, 1H), 7.79 (t, J = 7.8 Hz, 1H), 7.57 (t, J = 7.5 Hz, 1H), 6.59 (s, 1H), 4.06 (s, 3H), 3.95 (s, 3H), 2.53 (s, 3H). MS (ESI, $[M + H]^+$) m/z 310.3.

5-(4-Bromobutoxy)-2-methylfuro[3,2-*c*]phenanthridine-10,11-dione (21a) and 4-(4-Bromobutyl)-2-methylfuro[3,2-*c*]phenanthridine-5,10,11(4*H*)-trione (21d). A mixture of **19** (154 mg, 0.5 mmol), 1,4-dibromobutane (860 mg, 4.0 mmol) and K_2CO_3 (142 mg, 1.0 mmol) in anhydrous DMF (4 mL) was stirred at 80 °C for 3 h. The reaction mixture was diluted with H_2O, and extracted with Et_2O (30 mL × 3). The combined organic layer was washed with brine, dried over anhydrous Na_2SO_4, and

concentrated *in vacuo* to give a dark red residue. The residue was further purified by silica gel column; elution with 20% EtOAc in hexane afforded the desired products **20a** (44 mg, 20%) and **20d** (62 mg, 28%) as colorless gel, respectively. Compound **20a**: ^{1}H NMR (300 MHz, $CDCl_3$) δ 9.44 (d, *J* = 8.6 Hz, 1H), 8.42 (d, *J* = 8.2 Hz, 1H), 7.81 (t, *J* = 7.6 Hz, 1H), 7.62 (t, *J* = 7.5 Hz, 1H), 6.64 (s, 1H), 4.78 (t, *J* = 5.6 Hz, 2H), 4.14 (s, 3H), 3.98 (s, 3H), 3.59 (t, *J* = 6.3 Hz, 2H), 2.61 (s, 3H), 2.17 (m, 4H). Compound **20d**: ^{1}H NMR (300 MHz, $CDCl_3$) δ 9.17 (d, *J* = 8.5 Hz, 1H), 8.49 (d, *J* = 7.8 Hz, 1H), 7.62 (t, *J* = 7.2 Hz, 1H), 7.44 (t, *J* = 7.4 Hz, 1H), 6.50 (s, 1H), 4.68 (m, 2H), 3.97 (s, 3H), 3.79 (s, 3H), 3.42 (m, 2H), 2.44 (m, 3H), 1.98 (m, 4H).

Following a similar synthetic procedure to the preparation of **21c** provided compounds **21a** (30 mg, 72%) and **21d** (56 mg, 97%) as red solids from **20a** and **20d**, respectively. Compound **21a**: ^{1}H NMR (300 MHz, $CDCl_3$) δ 9.22 (d, *J* = 8.6 Hz, 1H), 8.16 (d, *J* = 8.3 Hz, 1H), 7.77 (t, *J* = 7.8 Hz, 1H), 7.51 (t, *J* = 7.6 Hz, 1H), 6.38 (s, 1H), 4.69 (t, *J* = 5.5 Hz, 2H), 3.58 (t, *J* = 6.0 Hz, 2H), 2.43 (s, 3H), 2.15 (m, 4H). Compound **21d**: ^{1}H NMR (300 MHz, $CDCl_3$) δ 9.13 (d, *J* = 8.5 Hz, 1H), 8.38 (d, *J* = 8.1 Hz, 1H), 7.75 (t, *J* = 7.8 Hz, 1H), 7.52 (t, *J* = 7.5 Hz, 1H), 6.58 (s, 1H), 4.66 (m, 2H), 3.53 (m, 2H), 2.54 (s, 3H), 2.08 (m, 4H).

5-((5-Bromopentyl)oxy)-2-methylfuro[3,2-*c*]phenanthridine-10,11-dione (21b) and 4-(5-bromopentyl)-2-methylfuro[3,2-*c*]phenanthridine-5,10,11(4*H*)-trione (21e). A mixture of **19** (154 mg, 0.5 mmol), 1,5-dibromopentane (900 mg, 4.0 mmol) and K_2CO_3 (142 mg, 1.0 mmol) in anhydrous DMF (4 mL) was stirred at 80 °C for 3 h. The reaction mixture was diluted with H_2O, and extracted with Et_2O (30 mL × 3).

The combined organic layer was washed with brine, dried over anhydrous Na_2SO_4, and concentrated *in vacuo* to give a dark red residue. The residue was further purified by silica gel column; elution with 20% EtOAc in hexane afforded the desired products **20b** (55 mg, 24%) and **20e** (75 mg, 33%) as colorless gel, respectively. Compound **20b**: ^{1}H NMR (300 MHz, $CDCl_3$) δ 9.44 (d, *J* = 8.7 Hz, 1H), 8.43 (d, *J* = 8.0 Hz, 1H), 7.80 (t, *J* = 7.8 Hz, 1H), 7.66 – 7.57 (t, *J* = 6.9 Hz, 1H), 6.64 (s, 1H), 4.75 (t, *J* = 6.4 Hz, 2H), 4.13 (s, 3H), 3.98 (s, 3H), 3.50 (t, *J* = 6.8 Hz, 2H), 2.61 (s, 3H), 2.10 – 1.97 (m, 4H), 1.83 – 1.73 (m, 2H). Compound **20e**: ^{1}H NMR (300 MHz, $CDCl_3$) δ 9.27 (d, *J* = 8.5 Hz, 1H), 8.59 (d, *J* = 7.9 Hz, 1H), 7.72 (t, *J* = 7.8 Hz, 1H), 7.54 (t, *J* = 7.5 Hz, 1H), 6.60 (s, 1H), 4.83 – 4.69 (m, 2H), 4.06 (t, *J* = 7.5 Hz, 3H), 3.89 (s, 3H), 3.46 (t, *J* = 6.7 Hz, 2H), 2.54 (s, 3H), 2.04 – 1.87 (m, 4H), 1.68 (m, 2H).

Following a similar synthetic procedure to the preparation of **21c**, compounds **21b** (31 mg, 60%) and **21e** (69 mg, 98%) was obtained from **20b** and **20e** as red solids, respectively. Compound **21b**: ^{1}H NMR (300 MHz, $CDCl_3$) δ 9.24 (d, *J* = 8.6 Hz, 1H), 8.18 (d, *J* = 8.3 Hz, 1H), 7.78 (t, *J* = 7.8 Hz, 1H), 7.52 (t, *J* = 7.6 Hz, 1H), 6.40 (s, 1H), 4.68 (t, *J* = 6.4 Hz, 2H), 3.49 (t, *J* = 6.6 Hz, 2H), 2.44 (s, 3H), 2.09 – 1.93 (m, 4H), 1.73 (m, 2H). Compound **21e**: ^{1}H NMR (300 MHz, $CDCl_3$) δ 9.13 (d, *J* = 8.5 Hz, 1H), 8.38 (d, *J* = 8.0 Hz, 1H), 7.75 (t, *J* = 7.8 Hz, 1H), 7.52 (t, *J* = 7.6 Hz, 1H), 6.58 (s, 1H), 4.70 – 4.58 (d, *J* = 7.8 Hz, 2H), 3.48 (t, *J* = 6.4 Hz, 2H), 2.53 (s, 3H), 1.94 (m, 4H), 1.70 (m, 2H).

4-(3-Bromopropyl)-2-methylfuro[3,2-*c*]phenanthridine-5,10,11(4*H*)-trione (21c). A mixture of **19** (309 mg, 1.0 mmol), 1,3-dibromopropane (1.728 g, 8.0 mmol) and

K_2CO_3 (276 mg, 2.0 mmol) in anhydrous DMF (8 mL) was stirred at 80 °C for 3 h. The reaction mixture was diluted with H_2O, and extracted with Et_2O (30 mL × 3). The combined organic layer was washed with brine, dried over anhydrous Na_2SO_4, and concentrated *in vacuo* to give a dark red residue. The residue was further purified by silica gel column; elution with 20% EtOAc in hexane afforded the desired product **20c** as colorless solid (296 mg, 69% yield). ^{1}H NMR (300 MHz, $CDCl_3$) δ 9.25 (d, *J* = 8.5 Hz, 1H), 8.56 (d, *J* = 7.8 Hz, 1H), 7.72 (t, *J* = 7.5 Hz, 1H), 7.53 (t, *J* = 7.5 Hz, 1H), 6.59 (s, 1H), 4.94 – 4.84 (t, *J* = 9.0 Hz, 2H), 4.06 (s, 3H), 3.88 (s, 3H), 3.62 (t, *J* = 6.7 Hz, 2H), 2.58 – 2.43 (m, 5H).

To a solution of **20c** (0.05 mmol) in anhydrous CH_2Cl_2 (2 mL) was added dropwise a solution of BBr_3 in CH_2Cl_2 (1.2 M，0.25 mL) at -55 °C. The resulting reaction mixture was stirred at rt for 8 h, and then was quenched by anhydrous MeOH. The resulting mixture was then stirred at rt under air overnight, and then washed with brine, dried over anhydrous Na_2SO_4, and concentrated *in vacuo* to give a dark red residue. The residue was further purified by silica gel column; elution with 25% EtOAc in hexane afforded the desired product **21c** as colorless solid in 92% yield. ^{1}H NMR (400 MHz, $CDCl_3$) δ 9.16 (d, *J* = 8.5 Hz, 1H), 8.41 (d, *J* = 8.1 Hz, 1H), 7.78 (t, *J* = 7.8 Hz, 1H), 7.54 (t, *J* = 7.6 Hz, 1H), 6.60 (s, 1H), 4.84 – 4.78 (m, 2H), 3.65 (t, *J* = 6.3 Hz, 2H), 2.56 (s, 3H), 2.49 (m, 2H).

4-(2-Hydroxyethyl)-2-methylfuro[3,2-*c*]phenanthridine-5,10,11(4*H*)-trione (21f), 5-(2-hydroxyethoxy)-2-methylfuro[3,2-*c*]phenanthridine-10,11-dione (21g), and 5-(2-(2-bromoethoxy)ethoxy)-2-methylfuro[3,2-*c*]phenanthridine-10,11(3b*H*,9b*H*

)-dione (21h). A mixture of **19** (154 mg, 0.5 mmol), 1-bromo-2-(2-bromoethoxy)ethane (1080 mg, 4.6 mmol) and K_2CO_3 (142 mg, 1.0 mmol) in anhydrous DMF (4 mL) was stirred at 80 °C for 3 h. The reaction mixture was diluted with H_2O, and extracted with Et_2O (30 mL × 3). The combined organic layer was washed with brine, dried over anhydrous Na_2SO_4, and concentrated *in vacuo* to give a dark red residue. The residue was further purified by silica gel column; elution with 20% EtOAc in hexane afforded the desired products **20f** (98 mg, 43%) and **20g** (90 mg, 39%) as colorless gel, respectively. Compound **20f**: ^{1}H NMR (300 MHz, $CDCl_3$) δ 9.23 (d, *J* = 8.5 Hz, 1H), 8.54 (d, *J* = 7.9 Hz, 1H), 7.69 (t, *J* = 7.8 Hz, 1H), 7.50 (t, *J* = 7.5 Hz, 1H), 6.57 (s, 1H), 5.03 (t, *J* = 6.8 Hz, 2H), 4.03 (s, 3H), 3.93 (t, *J* = 6.8 Hz, 2H), 3.85 (m, 5H), 3.41 (t, *J* = 6.1 Hz, 2H). Compound **20g**: ^{1}H NMR (300 MHz, $CDCl_3$) δ 9.44 (d, *J* = 8.6 Hz, 1H), 8.46 (d, *J* = 8.1 Hz, 1H), 7.81 (t, *J* = 7.8 Hz, 1H), 7.62 (t, *J* = 7.6 Hz, 1H), 6.64 (s, 1H), 4.97 – 4.90 (t, *J* = 4.8 Hz, 2H), 4.13 (s, 3H), 4.09 – 4.05 (t, *J* = 5.1 Hz, 2H), 3.96 (m, 5H), 3.52 (t, *J* = 6.3 Hz, 2H), 2.59 (s, 3H).

Following a similar synthetic procedure to the preparation of **21c**, treating **20f** with BBr_3 at -55 °C produced **21f** (20 mg, 29%) as red solids; while treating **20g** with BBr_3 at -55 °C provided compound **21g** (40 mg, 63%) together with **21h** (60 mg, 71%) as red solids. Compound **21f**: Mp: 208−209 °C. HPLC purity: 96.5%. ^{1}H NMR (300 MHz, DMSO) δ 9.06 (d, *J* = 9.0 Hz, 1H), 8.29 (d, *J* = 8.0 Hz, 1H), 7.83 (t, *J* = 7.9 Hz, 1H), 7.58 (t, *J* = 7.5 Hz, 1H), 6.74 (s, 1H), 4.94 (t, *J* = 5.6 Hz, 1H), 4.78 (t, *J* = 6.7 Hz, 2H), 3.72 (q, *J* = 6.1 Hz, 2H), 2.48 (s, 3H). ^{13}C NMR (126 MHz, DMSO) δ 179.63,

173.95, 162.05, 157.98, 151.96, 140.29, 134.54, 134.09, 128.17, 128.14, 126.14, 125.47, 123.85, 108.03, 105.70, 59.58, 48.25, 13.83. MS (ESI, $[M + H]^+$) m/z 324.2. HRMS (ESI) calcd for $C_{18}H_{14}NO_5$, 324.0866; found, 324.0873. Compound **21g**: Mp: 207−208 °C. HPLC purity: 97.0%. ^{1}H NMR (300 MHz, DMSO) δ 9.20 (d, *J* = 7.2 Hz, 1H), 8.35 (d, *J* = 7.3 Hz, 1H), 7.97 – 7.90 (d, *J* = 7.2 Hz, 1H), 7.68 (t, *J* = 7.7 Hz, 1H), 6.64 (s, 1H), 5.05 (t, *J* = 5.5 Hz, 1H), 4.68 (t, *J* = 4.7 Hz, 2H), 3.90 (q, *J* = 4.8 Hz, 2H), 2.46 (s, 3H); ^{13}C NMR (126 MHz, DMSO) δ 181.01, 174.00, 164.18, 157.91, 157.43, 144.62, 136.29, 134.62, 128.20, 125.44, 125.38, 123.81, 118.96, 113.40, 105.46, 69.85, 59.63, 13.93. MS (ESI, $[M + H]^+$) m/z 324.3. HRMS (ESI) calcd for $C_{18}H_{13}NNaO_5$, 346.0686; found, 346.0693. Compound **21h**: ^{1}H NMR (300 MHz, $CDCl_3$) δ 9.29 (d, *J* = 8.7 Hz, 1H), 8.29 (d, *J* = 8.4 Hz, 1H), 7.82 (t, *J* = 7.8 Hz, 1H), 7.56 (t, *J* = 7.6 Hz, 1H), 6.45 (s, 1H), 4.95 – 4.86 (t, *J* = 4.2 Hz, 2H), 4.10 – 4.02 (t, *J* = 3.9 Hz, 2H), 3.96 (t, *J* = 6.0 Hz, 2H), 3.53 (t, *J* = 5.9 Hz, 2H), 2.47 (s, 3H).

General Experimental Procedure for Synthesis of Compounds 22a-n:

A mixture of the bromo *o*-quinones **21a-e** and **21h** (0.05 mmol), various secondary amines (0.3 mmol) and K_2CO_3 (0.1 mmol) in anhydrous DMF (2 mL) was stirred at 40 °C for 12 h. The reaction mixture was diluted with H_2O, and extracted with CH_2Cl_2 (30 mL × 3). The combined organic layer was washed with brine, dried over anhydrous Na_2SO_4, and concentrated *in vacuo* to give a dark red residue. The residue was further purified by silica gel column; elution with 2-5% MeOH in CH_2Cl_2 afforded the final products **22a-n** in 44-88% yields as red solids.

5-(4-(Dimethylamino)butoxy)-2-methylfuro[3,2-*c*]phenanthridine-10,11-dione (22a): Yield: 54%. Mp: 207−208 °C. HPLC purity: 96.0%. ^{1}H NMR (300 MHz, $CDCl_3$) δ 9.26 (d, *J* = 8.6 Hz, 1H), 8.23 (d, *J* = 8.3 Hz, 1H), 7.79 (t, *J* = 7.9 Hz, 1H), 7.54 (t, *J* = 7.6 Hz, 1H), 6.43 (s, 1H), 4.74 (t, *J* = 6.3 Hz, 2H), 2.57 – 2.49 (t, *J* = 7.2 Hz, 2H), 2.46 (s, 3H), 2.36 (s, 6H), 1.99 (m, 2H), 1.83 (m, 2H); ^{13}C NMR (126 MHz, $CDCl_3$) δ 181.28, 174.21, 164.72, 158.79, 157.19, 145.25, 136.37, 134.10, 127.71, 125.79, 124.82, 123.35, 119.27, 113.08, 104.98, 67.66, 59.13, 45.14, 26.69, 24.01, 13.85, 6.81. MS (ESI, $[M + H]^+$) m/z 379.3. HRMS (ESI) calcd for $C_{22}H_{23}N_2O_4$, 379.1652; found, 379.1648.

5-((5-(Dimethylamino)pentyl)oxy)-2-methylfuro[3,2-*c*]phenanthridine-10,11-dione (22b): Yield: 64%. Mp: 209−210 °C. HPLC purity: 98.7%. ^{1}H NMR (300 MHz, $CDCl_3$) δ 9.26 (d, *J* = 8.7 Hz, 1H), 8.23 (d, *J* = 8.1 Hz, 1H), 7.80 (t, *J* = 7.8 Hz, 1H), 7.54 (t, *J* = 7.7 Hz, 1H), 6.43 (s, 1H), 4.73 (t, *J* = 6.2 Hz, 2H), 2.75 – 2.66 (t, *J* = 6.0 Hz, 2H), 2.54 (s, 6H), 2.47 (s, 3H), 2.00 (m, 2H), 1.84 (m, 2H), 1.65 (m, 2H); ^{13}C NMR (126 MHz, $CDCl_3$) δ 181.30, 174.21, 164.69, 158.77, 157.23, 145.24, 136.38, 134.12, 127.73, 125.81, 124.80, 123.36, 119.24, 113.09, 104.98, 67.54, 58.83, 44.22 (2C), 28.58, 25.89, 23.80, 13.87. MS (ESI, $[M + H]^+$) m/z 393.4. HRMS (ESI) calcd for $C_{23}H_{25}N_2O_4$, 393.1809; found, 393.1802.

4-(4-(Dimethylamino)butyl)-2-methylfuro[3,2-*c*]phenanthridine-5,10,11(4*H*)-trione (22c): Yield: 86%. Mp: 205−206 °C. HPLC purity: 98.0%. ^{1}H NMR (300 MHz, $CDCl_3$) δ 9.15 (d, *J* = 8.4 Hz, 1H), 8.41 (d, *J* = 8.0 Hz, 1H), 7.76 (t, *J* = 7.7 Hz, 1H), 7.53 (t, *J* = 7.4 Hz, 1H), 6.59 (s, 1H), 4.73 – 4.61 (d, *J* = 7.2 Hz, 2H), 2.51 (s, 3H),

2.47 – 2.38 (d, *J* = 7.2 Hz, 2H), 2.29 (s, 6H), 1.89 (m, 2H), 1.72 (m, 2H); ^{13}C NMR (126 MHz, $CDCl_3$) δ 179.55, 174.02, 162.28, 157.46, 152.14, 139.36, 134.43, 133.64, 128.18 (2C), 126.43, 125.33, 124.06, 108.45, 105.89, 59.19, 47.00, 45.27 (2C), 27.71, 24.95, 13.91. MS (ESI, $[M + H]^+$) m/z 379.3. HRMS (ESI) calcd for $C_{22}H_{23}N_2O_4$, 379.1652; found, 379.1650.

4-(5-(Dimethylamino)pentyl)-2-methylfuro[3,2-*c*]phenanthridine-5,10,11(4*H*)-trione (22d): Yield: 50%. Mp: 204−205 °C. HPLC purity: 97.4%. ^{1}H NMR (300 MHz, $CDCl_3$) δ 9.16 (d, *J* = 8.8 Hz, 1H), 8.40 (d, *J* = 7.9 Hz, 1H), 7.76 (t, *J* = 7.7 Hz, 1H), 7.53 (t, *J* = 7.5 Hz, 1H), 6.59 (s, 1H), 4.66 (d, *J* = 7.5 Hz, 2H), 2.55 – 2.43 (m, 5H), 2.36 (s, 6H), 1.89 (m, 2H), 1.70 (m, 2H), 1.57 (m, 2H). ^{13}C NMR (126 MHz, $CDCl_3$) δ 179.57, 173.94, 162.41, 157.73, 151.92, 139.25, 134.53, 133.68, 128.23, 128.11, 126.51, 125.41, 123.97, 108.54, 105.93, 58.21, 46.59, 43.44 (2C), 29.16, 24.69, 24.22, 14.01. MS (ESI, $[M + H]^+$) m/z 393.4. HRMS (ESI) calcd for $C_{23}H_{25}N_2O_4$, 393.1809; found, 393.1805.

4-(3-(Dimethylamino)propyl)-2-methylfuro[3,2-*c*]phenanthridine-5,10,11(4*H*)-trione (22e): Yield: 79%. Mp: 203−204 °C. HPLC purity: 97.6%. ^{1}H NMR (300 MHz, $CDCl_3$) δ 9.16 (d, *J* = 8.7 Hz, 1H), 8.42 (d, *J* = 8.2 Hz, 1H), 7.77 (t, *J* = 7.7 Hz, 1H), 7.54 (t, *J* = 7.7 Hz, 1H), 6.59 (s, 1H), 4.79 – 4.66 (t, *J* = 7.5 Hz, 2H), 2.58 – 2.48 (m, 5H), 2.29 (s, 6H), 2.12 – 2.01 (m, 2H); ^{13}C NMR (126 MHz, $CDCl_3$) δ 180.29, 174.76, 163.06, 158.08, 152.98, 140.24, 135.12, 134.37, 128.86, 127.15, 125.95, 124.78, 109.20, 106.58, 57.82, 46.51, 46.17 (2C), 30.41, 28.28, 14.61. MS (ESI, $[M + H]^+$) m/z 365.3. HRMS (ESI) calcd for $C_{21}H_{21}N_2O_4$, 365.1496; found, 365.1500.

4-(3-(Diethylamino)propyl)-2-methylfuro[3,2-*c*]phenanthridine-5,10,11(4*H*)-trion e (22h). Yield: 65%. Mp: 203−204 °C. HPLC purity: 98.2%. ^{1}H NMR (300 MHz, $CDCl_3$) δ 9.13 (d, *J* = 8.5 Hz, 1H), 8.38 (d, *J* = 8.1 Hz, 1H), 7.76 (t, *J* = 7.7 Hz, 1H), 7.52 (t, *J* = 7.4 Hz, 1H), 6.56 (s, 1H), 4.68 (t, *J* = 7.4 Hz, 2H), 2.85 (m, 6H), 2.57 (s, 3H), 2.25 (m, 2H), 1.20 (t, *J* = 6.9 Hz, 6H); ^{13}C NMR (126 MHz, $CDCl_3$) δ 179.49, 173.83, 162.45, 158.00, 151.86, 139.33, 134.51, 133.65, 128.20, 128.08, 126.46, 125.39, 123.93, 108.45, 105.88, 50.06, 46.61 (2C), 45.57, 26.23, 14.06, 10.34 (2C).MS (ESI, $[M + H]^+$) m/z 393.4. HRMS (ESI) calcd for $C_{23}H_{25}N_2O_4$, 393.1809; found, 393.1807.

2-Methyl-4-(3-(pyrrolidin-1-yl)propyl)furo[3,2-*c*]phenanthridine-5,10,11(4*H*)-tri one (22f): Yield: 44%. Mp: 205−206 °C. HPLC purity: 97.8%. ^{1}H NMR (300 MHz, $CDCl_3$) δ 9.13 (d, *J* = 8.4 Hz, 1H), 8.38 (d, *J* = 7.9 Hz, 1H), 7.76 (t, *J* = 7.3 Hz, 1H), 7.52 (t, *J* = 7.4 Hz, 1H), 6.55 (s, 1H), 4.74 (d, *J* = 7.2 Hz, 2H), 2.93 (m, 6H), 2.56 (s, 3H), 2.37 – 2.28 (m, 2H), 1.93 (m, 4H); ^{13}C NMR (126 MHz, $CDCl_3$) δ 179.46, 173.71, 162.56, 158.28, 151.72, 139.32, 134.58, 133.62, 128.23, 128.07, 126.46, 125.37, 123.82, 108.43, 105.82, 53.89, 53.45, 45.18, 29.71, 27.43, 23.41 (2C), 14.11. MS (ESI, $[M + H]^+$) m/z 391.3. HRMS (ESI) calcd for $C_{23}H_{23}N_2O_4$, 391.1652; found, 391.1647.

2-Methyl-4-(3-(piperidin-1-yl)propyl)furo[3,2-*c*]phenanthridine-5,10,11(4*H*)-trio ne (22g). Yield: 62%. Mp: 203−204 °C. HPLC purity: 97.2%. ^{1}H NMR (300 MHz, $CDCl_3$) δ 9.16 (d, *J* = 8.0 Hz, 1H), 8.40 (d, *J* = 8.0 Hz, 1H), 7.75 (t, *J* = 8.6 Hz, 1H), 7.54 (t, *J* = 7.1 Hz, 1H), 6.58 (s, 1H), 4.72 (t, *J* = 6.9 Hz, 2H), 2.78 – 2.00 (m, 11H),

1.54 (m, 6H); ^{13}C NMR (126 MHz, CD_3OD) δ 179.43, 173.64, 162.61, 162.56, 158.20, 152.00, 139.86, 133.86, 127.58, 127.52, 125.94, 125.35, 123.74, 108.08, 104.96, 55.91, 53.99 (2C), 45.29, 25.53, 24.76 (2C), 23.33, 12.28. MS (ESI, $[M + H]^+$) m/z 405.3. HRMS (ESI) calcd for $C_{24}H_{25}N_2O_4$, 405.1809; found, 405.1806.

2-Methyl-4-(3-(4-methylpiperazin-1-yl)propyl)furo[3,2-c]phenanthridine-5,10,11 (4*H*)-trione (22i): Yield: 88%. Mp: 201−203 °C. HPLC purity: 98.0%. ^{1}H NMR (300 MHz, $CDCl_3$) δ 9.15 (d, *J* = 8.6 Hz, 1H), 8.40 (d, *J* = 7.9 Hz, 1H), 7.76 (t, *J* = 7.7 Hz, 1H), 7.53 (t, *J* = 7.5 Hz, 1H), 6.59 (s, 1H), 4.81 – 4.66 (d, *J* = 6.6 Hz, 2H), 2.63 – 2.32 (m, 11H), 2.26 (s, 3H), 2.14 – 1.97 (m, 4H); ^{13}C NMR (126 MHz, $CDCl_3$) δ 179.54, 174.03, 162.37, 157.32, 152.30, 139.56, 134.41, 133.65, 128.17, 126.42, 125.25, 124.07, 108.48, 105.89, 55.95, 54.92, 53.08, 45.90, 45.72 (2C), 26.65 (2C), 20.07, 13.94. MS (ESI, $[M + H]^+$) m/z 420.4. HRMS (ESI) calcd for $C_{24}H_{26}N_3O_4$, 420.1918; found, 420.1925.

2-Methyl-4-(3-morpholinopropyl)furo[3,2-*c*]phenanthridine-5,10,11(4*H*)-trione (22j): Yield: 86%. Mp: 203−204 °C. HPLC purity: 97.8%. ^{1}H NMR (300 MHz, $CDCl_3$) δ 9.06 (d, *J* = 7.9 Hz, 1H), 8.31 (d, *J* = 7.8 Hz, 1H), 7.68 (t, *J* = 6.9 Hz, 1H), 7.45 (t, *J* = 7.0 Hz, 1H), 6.51 (s, 1H), 4.65 (m, 2H), 3.60 (m, 4H), 2.47 (m, 9H), 2.02 (m, 2H); ^{13}C NMR (126 MHz, $CDCl_3$) δ 180.12, 174.59, 163.14, 158.30, 152.82, 140.16, 135.17, 134.25, 128.92, 128.73, 127.03, 125.94, 124.59, 109.12, 106.53, 68.23, 56.93, 54.21 (2C), 46.33, 30.34, 26.84, 14.49. MS (ESI, $[M + H]^+$) m/z 407.3. HRMS (ESI) calcd for $C_{23}H_{23}N_2O_5$, 407.1601; found, 407.1606.

2-Methyl-4-(3-(4-morpholinopiperidin-1-yl)propyl)furo[3,2-*c*]phenanthridine-5,10,11(4*H*)-trione (22k). Yield: 55%. Mp: 203−205 °C. HPLC purity: 97.2%. ^{1}H NMR (300 MHz, $CDCl_3$) δ 9.13 (d, *J* = 8.6 Hz, 1H), 8.38 (d, *J* = 8.1 Hz, 1H), 7.74 (t, *J* = 7.4 Hz, 1H), 7.51 (t, *J* = 7.2 Hz, 1H), 6.57 (s, 1H), 4.70 (m, 2H), 3.70 (m, 4H), 2.99 (m, 2H), 2.51 (m, 8H), 1.96 (m, 8H), 1.44 (m, 2H); ^{13}C NMR (126 MHz, $CDCl_3$) δ 184.11, 178.54, 167.26, 162.60, 156.77, 144.24, 139.12, 138.24, 132.87, 132.67, 130.97, 129.92, 128.47, 113.05, 110.37, 71.42 (2C), 60.20, 60.00, 57.38, 54.12 (2C), 50.25, 50.01, 31.76, 31.07,18.28 (2C). MS (ESI, $[M + H]^+$) m/z 490.4. HRMS (ESI) calcd for $C_{28}H_{32}N_3O_5$, 490.2336; found, 490.2339.

4-(3-(4-(2-Hydroxyethyl)piperidin-1-yl)propyl)-2-methylfuro[3,2-*c*]phenanthridine-5,10,11(4*H*)-trione (22l): Yield: 53%. Mp: 206−207 °C. HPLC purity: 97.7%. ^{1}H NMR (300 MHz, $CDCl_3$) δ 9.10 (d, *J* = 7.8 Hz, 1H), 8.35 (d, *J* = 7.7 Hz, 1H), 7.76 (t, *J* = 7.0 Hz, 1H), 7.53 (t, *J* = 7.6 Hz, 1H), 6.57 (s, 1H), 4.68 (m, 2H), 3.92 (m, 2H), 3.63 (m, 2H), 3.24 (s, 1H), 2.86 (m, 1H), 2.43 (m, 7H), 1.81 (m, 2H), 1.53 (m, 5H); ^{13}C NMR (126 MHz, $CDCl_3$) δ 180.11, 174.45, 163.25, 158.84, 152.54, 140.08, 135.21, 134.25, 128.90, 128.70, 127.00, 125.99, 124.43, 109.07, 106.42, 60.17 (2C), 56.25, 54.23, 45.96 (2C), 39.02, 32.12, 30.32, 26.33, 14.51. MS (ESI, $[M + H]^+$) m/z 449.4. HRMS (ESI) calcd for $C_{26}H_{29}N_2O_5$, 449.2071; found, 449.2068.

4-(3-(1*H*-Imidazol-1-yl)propyl)-2-methylfuro[3,2-*c*]phenanthridine-5,10,11(4*H*)-trione (22m): Yield: 82%. Mp: 205−206 °C. HPLC purity: 98.4%. ^{1}H NMR (500 MHz, DMSO) δ 9.03 (s, 1H), 8.26 (s, 1H), 7.86 (s, 1H), 7.81(s, 1H), 7.57 (s, 1H), 7.33 (s, 1H), 7.00 (s, 1H), 6.73 (s, 1H), 4.53 (s, 2H), 4.20 (s, 2H), 2.43 (s, 3H), 2.26 (s,

2H); ^{13}C NMR (126 MHz, DMSO) δ 181.38, 175.72, 163.81, 160.14, 153.43, 141.73, 139.51(2C), 136.47, 135.92, 130.05, 129.96, 127.99, 127.43, 125.63, 122.03, 109.93, 107.71, 46.97, 46.61, 32.71, 15.66. MS (ESI, $[M + H]^+$) m/z 388.3. HRMS (ESI) calcd for $C_{22}H_{18}N_3O_4$, 388.1292; found, 388.1295.

5-(2-(2-(Dimethylamino)ethoxy)ethoxy)-2-methylfuro[3,2-*c*]phenanthridine-10,11-dione (22n): Yield: 35%. Mp: 206−207 °C. HPLC purity: 96.5%. ^{1}H NMR (300 MHz, $CDCl_3$) δ 9.28 (d, *J* = 8.6 Hz, 1H), 8.28 (d, *J* = 8.3 Hz, 1H), 7.81 (t, *J* = 7.4 Hz, 1H), 7.55 (t, *J* = 7.4 Hz, 1H), 6.45 (s, 1H), 4.90 (t, *J* = 6.0 Hz, 2H), 4.00 (t, *J* = 3.0 Hz, 2H), 3.77 (t, *J* = 5.4 Hz, 2H), 2.64 (t, *J* = 5.4 Hz, 2H), 2.47 (s, 3H), 2.35 (s, 6H); ^{13}C NMR (126 MHz, $CDCl_3$) δ 181.32, 174.17, 164.50, 158.74, 157.22, 145.05, 136.44, 134.20, 127.76, 125.79, 124.94, 123.38, 119.23, 113.27, 105.01, 69.19, 69.12, 66.91, 58.66, 45.64 (2C), 13.84. MS (ESI, $[M + H]^+$) m/z 395.4. HRMS (ESI) calcd for $C_{22}H_{23}N_2O_5$, 395.1601; found, 395.1598.

Tested Compounds and Antibodies: All tested compounds were dissolved in dimethyl sulfoxide (DMSO), aliquoted, stored at -20 °C and diluted to desired concentrations in normal saline immediately prior to each experiment. The final DMSO concentration did not exceed 0.1%. Compound **1** was purchased from Selleck (Houston, TX, USA). Z-VAD-FMK was from MedChemExpress (NJ, USA). The AnnexinV-FITC/PI apoptosis detection kit was from Keygen (Nanjing, China). Primary antibodies against Caspase 3, Caspase 7 and PARP1, respectively, were all from Cell Signaling Technology (Danvers, MA).

Cell Culture: HUVEC, A549, H460, HCT-116, BT-474, DU-145, HepG, BEL7404, MGC803, and KB cancer cell lines were purchased from American Type Culture Collection (ATCC, Manassas, VA). The multidrug resistance (MDR) cell line KB/VCR was obtained from Zhongshan University of Medical Sciences (Guangzhou, China). Cells were normally cultured in the ATCC-specified medium supplemented with 10% heat-inactivated fetal bovine serum (GIBCO), penicillin (100 IU/mL), streptomycin (100 μg/mL) and Hepes (10 mM) in a humidified atmosphere containing 5% CO_2 at 37 °C. All cells were periodically authenticated by morphologic inspection and tested for Mycoplasma contamination.

Proliferative Inhibition Assays: Cells were seeded into 96-well plates, cultured overnight and treated with gradient concentrations of the tested agents for 72 h. The IC_{50} values of different agents were measured by the sulforhodamine B (SRB; Sigma, MO). The proliferative inhibition rate (%) was calculated as: $[1-(A450_{treated}/A450_{control})] \times 100\%$. The averaged IC_{50} values (mean ± SE) were determined with the Logit method from three independent tests.

Liver Microsomal Stability Assays: The incubation is performed as follows: microsomes in 0.1 M Tris/HCl buffer pH 7.4 (0.33 mg/mL microsomal protein), co-factor $MgCl_2$ (5 mM), tested compound (final concentration 0.1 μM, co-solvent (0.01% DMSO) and 0.005% Bovin serum albumin) and NADPH (1 mM) at 37 °C for 60 min. The reaction can be started by the addition of liver microsomes, or the tested compound or NADPH. Aliquots were sampled at 0, 7, 17, 30 and 60 min incubation

and enzymatic reaction was stopped by protein precipitation in methanol. After centrifugation, samples were then analyzed by LC-MS/MS.

Annexin V-FITC/PI Apoptosis Assays: HCT-116 cells were seeded into 6-well plates, cultured overnight and treated with **22h** or **1** for the indicated time were collected and washed with PBS. Then, cells were co-stained with Annexin V-FITC and PI according to the kit instruction. Cell apoptosis was detected with a FACS Calibur cytometer (BD Biosciences, San Jose, CA, USA). Samples were analyzed by flow cytometry, and 10000 events were counted each time.

Western Blotting: HCT116 cells treated with **22h** or **1** for the indicated time were collected for Western blotting. Cell lysates were prepared in lysis buffer (2 mM sodium orthovanadate, 50 mM NaF, 20 mM Hepes, 150 mM NaCl, 1.5 mM $MgCl_2$, 5 mM sodium pyrophosphate, 10% glycerol, 0.2% Triton X-100, 5 mM EDTA, 1 mM PMSF, 10 μg/ml leupeptin, and 10 μg/mL aprotinin) on ice for 30 min. Samples were clarified by centrifugation at 4 °C for 15 min at 12,000×g, and then equal amounts of protein were separated on SDS-polyacrylamide gels and transferred to nitrocellulose membranes. The blots were incubated overnight at 4 °C with the following polyclonal antibodies: anti-PARP (1:1000), anti-Caspase 7 (1:1000), anti-Caspase 3 (1:1000) or anti-β-Actin (1:2000). Bands were visualized using horseradish peroxidase-conjugated secondary antibodies (Calbiotech, San Diego, CA, USA, 1:2000) followed by enhanced chemiluminescence (Pierce Biotech, Rockford, IL,

USA), and then the protein bands were photographed (UVP, Gel Document System, GDS 8000, USA).

Caspase-Glo® 3/7 Assays: HCT116 cells were seeded into 96-well plates (5×10^3 per well) and incubated overnight. Then the cells were treated with compound **22h** or **1** for 24 h at 37°C. Caspase-Glo® 3/7 Reagent from Promega (Madison, WI) was added into the wells (100 μL per well). The cells were incubated with the reagent for 1 h at room temperature. The luminescence value of each sample was measured with an EnVision® Multilabel Reader (PerkinElmer).

***In Vivo* Antitumor Activity Determination:** Compound **22h** at the dose of 10 mg/kg (iv) and 30 mg/kg (ip) was selected for evaluating its *in vivo* antitumor activity. 5-FU at 15 mg/kg was used as the positive control. 1% DMSO in sterile saline was used as the vehicle. BALB/C nude male mice (certificate SCXK-2007-0005, weighing 18−20 g) were obtained from the Shanghai Experimental Animal Center, Chinese Academy of Sciences. HCT116 colon cancer cell suspensions were implanted subcutaneously into the right axilla region of the mice. Treatment began when implanted tumors had reached a volume greater than 100 mm^3 (after 14 days). The animals were randomized into appropriate groups (6 animals/treatment and 10 animals/control group) and administered by iv or ip injection of compound **22h** for 14 consecutive days once on day 14 after the implantation of cells. Observation was conducted after the first dosing and lasted over 18 days. Tumor volumes were monitored by caliper measurements of the length and width and calculated using the

formula of TV = 1/2 × a × b^2, where a is the tumor length, and b is the width. Tumor volumes and body weights were monitored every 4 days over the course of treatment. Mice were sacrificed on day 32 after the implantation of cells, and tumors were removed and recorded for analysis.

ASSOCIATED CONTENT

Supporting Information

The Supporting Information is available free of charge on the ACS Publications website at DOI: ^{1}H and ^{13}C NMR spectra for the target compounds**.**

AUTHOR INFORMATION

Corresponding Author

*Tel (A. Zhang): +86 (021) 50806035; Fax: +86 (021) 50806035; E-mail: aozhang@simm.ac.cn;

Tel (Z. Miao): +86 (021) 50806820; Fax: +86 (021) 50806820; E-mail: zhmiao@simm.ac.cn;

Tel (Y. Wang): +86 (021) 50806820; Fax: +86 (021) 50806820; E-mail: yqwang@simm.ac.cn.

Notes

C. Ding and Q. Tian contributed equally to this work. The authors declare no competing financial interest.

ACKNOWLEDGMENTS

This work was supported by grants from National Natural Science Foundation of China (81430080, 81373277, 81773565). Supporting from the National Program on

Key Basic Research Project of China (2015CB910603), the International Cooperative Program (GJHZ1622 2060899) and Key Program of the Frontier Science (QYZDJ-SSW-SMC002) of the Chinese Academy of Sciences, the Shanghai Commission of Science and Technology (16XD1404600, 14431905300 and 14431900400) were also appreciated.

ABBREVIATIONS USED

Tan-I, tanshinone I; Tan-IIA, tanshinone II; CPT, cryptotanshinone; TCM, traditional Chinese medicine; CFDA, China Food and Drug Administration; TMSI, trimethylsilyl iodide; HMBC, heteronuclear multiple bond correlation; SRB, sulforhodamine B; VCR, vincristine; HPLC, high performance liquid chromatography; PK, pharmacokinetic; PARP, poly (ADP-ribose) polymerase; SAR, structure-activity relationship; CK2α, Casein kinase 2, alpha 1; JAK3, Janus kinase 3.

REFERENCE:

1. a) Nakao, M.; Fukushima T. On the chemical composition of Salvia miltiorrhiza (Chinese drug Tan-shen) *J. Pharm. Soc. Jpn.* **1934**, *54*, 154–162; b) Dong, Y.; Morris-Natschke, S. L.; Lee, K. H. Biosynthesis, total syntheses, and antitumor activity of tanshinones and their analogs as potential therapeutic agents. *Nat. Prod. Rep.* **2011**, *28*, 529–542.

2. a) Shang, Q.; Xu, H.; Huang, L. Tanshinone IIA: a promising natural cardioprotective agent. *Evid. Based Complement Alternat. Med.* **2012**, *2012*, 716459; b) Gao, S.; Liu, Z.; Li, H.; Little, P. J.; Liu, P.; Xu, S. Cardiovascular actions and therapeutic potential of tanshinone IIA. *Atherosclerosis*, **2012**, *220*, 3–10; c) Kim, D. H.; Kim, S.; Jeon, S. J.; Son, K. H.; Lee, S.; Yoon, B. H.; Cheong, J. H.; Ko, K. H.; Ryu, J. H. Tanshinone I enhances learning and memory, and ameliorates memory impairment in mice via the extracellular signal-regulated kinase signalling pathway. *Br. J. Pharmacol.* **2009**, *158*, 1131–1142; d) Wang, X.; Bastow, K. F.; Sun, C. M.; Lin, Y. L.; Yu, H. J.; Don, M. J.; Wu, T. S.; Nakamura, S.; Lee, K. H. Antitumor Agents. 239. Isolation, structure elucidation, total synthesis, and anti-breast cancer activity of neo-tanshinlactone from Salvia miltiorrhiza. *J. Med. Chem.* **2004**, *47*, 5816–5819; e) Liu, W.; Zhou, J.; Geng, G.; Shi, Q.; Sauriol, F.; Wu, J. H. Antiandrogenic, maspin induction, and antiprostate cancer activities of tanshinone IIA and its novel derivatives with modification in ring A. *J. Med. Chem.* **2012**, *55*, 971-975; f) Dong, K.; Xu, W.; Yang, J.; Qiao, H.; Wu, L. Neuroprotective effects of Tanshinone IIA on permanent focal cerebral ischemia in mice. *Phytother. Res.* **2009**,

23, 608–613; g) Ren, Y.; Houghton, P. J.; Hider, R. C.; Howes, M. J. Novel diterpenoid acetylcholinesterase inhibitors from *Salvia miltiorhiza*. *Planta Med.* **2004**, *70*, 201–204; h) Wang, Q.; Yu, X.; Patal, K.; Hu, R.; Chuang, S.; Zhang, G.; Zheng, J. Tanshinones inhibit amyloid aggregation by amyloid-β peptide, disaggregate amyloid fibrils, and protect cultured cells. *ACS Chem. Neurosci.* **2013**, *4*, 1004–1015; i) Wang, D.; Lu, C.; Sun, F.; Cui, M.; Mu, H.; Duan, J.; Geng, H. A tanshinone I derivative enhances the activities of antibiotics against Staphylococcus aureus *in vitro* and *in vivo*. *Res. Microbiol.* **2017**, *168*, 46-54; j) Kim, S. Y.; Moon, T. C.; Chang, H. W.; Son, K. H.; Kang, S. S.; Kim, H. P. Effects of tanshinone I isolated from *Salvia miltiorrhiza* Bunge on arachidonic acid metabolism and *in vivo* inflammatory responses. *Phytother. Res.* **2002**, *16*, 616-620.

3. a) Zhang, Y.; Jiang, P.; Ye, M.; Kim, S.-H.; Jiang, C.; Lü, J. Tanshinones: sources, pharmacokinetics and anti-cancer activities. *Int. J. Mol. Sci.* **2012***, 13,* 13621-13666; b) Chen, X.; Guo, J.; Bao, J.; Lu, J.; Wang, Y. The anticancer properties of Salvia miltiorrhiza Bunge (Danshen): a systematic review. *Med. Res. Rev.* **2014**, *34*, 768-794;

4. a) Shin, E. A.; Sohn, E. J.; Won, G.; Choi, J. U.; Jeong, M.; Kim, B.; Kim, M. J.; Kim, S. H. Upregulation of microRNA135a-3p and death receptor 5 plays a critical role in tanshinone I sensitized prostate cancer cells to TRAIL induced apoptosis. *Oncotarget* **2014**, *5*, 5624-5636; b) Wang, L.; Wu, J.; Lu, J.; Ma, R.; Sun, D.; Tang, Regulation of the cell cycle and PI3K/Akt/mTOR signaling pathway by tanshinone I in human breast cancer cell lines. *J. Mol. Med. Rep.* **2015**, *11*, 931-939.

5. a) Xu, L.; Feng, J. M.; Li, J. X.; Zhu, J. M.; Song, S. S.; Tong, L. J.; Chen, Y.; Yang, X. Y.; Shen, Y. Y.; Lian, F. L.; Li, Y. P.; Lin, D. H.; Ding, J.; Miao, Z. H. Tanshinone-1 induces tumor cell killing, enhanced by inhibition of secondary activation of signaling networks. *Cell Death. Dis.* **2013**, *4*, e905; b) Nizamutdinova, I. T.; Lee, G. W.; Lee, J. S.; Cho, M. K.; Son, K. H.; Jeon, S. J.; Kang, S. S.; Kim, Y. S.; Lee, J. H.; Seo, H. G.; Chang, K. C.; Kim, H. J. Tanshinone I suppresses growth and invasion of human breast cancer cells, MDA-MB-231, through regulation of adhesion molecules. *Carcinogenesis* **2008**, *29*, 1885–1892; c) Wang, Y.; Li, J. X.; Wang, Y. Q.; Miao, Z. H. Tanshinone I inhibits tumor angiogenesis by reducing Stat3 phosphorylation at Tyr705 and hypoxia-induced HIF-1α accumulation in both endothelial and tumor cells. *Oncotarget* **2015**, *6*, 16031–16042.

6. a) Gong, Y.; Li, Y.; Lu, Y.; Li, L.; Abdolmaleky, H.; Blackburn, G. L.; Zhou, J. R. Bioactive tanshinones in Salvia miltiorrhiza inhibit the growth of prostate cancer cells in vitro and in mice. *Int. J. Cancer* **2011**, *129*, 1042–1052; b) Li, Y.; Gong, Y.; Li, L.; Abdolmaleky, H. M.; Zhou, J. R. Bioactive tanshinone I inhibits the growth of lung cancer in part via downregulation of Aurora A function. *Mol. Carcinog.* **2013**, *52*, 535-543; c) Tung, Y. T.; Chen, H. L.; Lee, C. Y.; Chou, Y. C.; Lee, P. Y.; Tsai, H. C.; Lin, Y. L.; Chen, C. M. Active component of Danshen (Salvia miltiorrhiza Bunge), tanshinone I, attenuates lung tumorigenesis via inhibitions of VEGF, cyclin A, and cyclin B expressions. *Evid. Based Complement Alternat. Med* .**2013**, *2013*, 319247.

7. a) Zheng, G.; Li, Z. Study on the anti-tumor effect and mechanism of tanshinone I. *J. Prac. Oncol.* **2005**, *94*, 33–35; b) Su, C. C.; Chen, G. W.; Lin, J. G. Growth

inhibition and apoptosis induction by tanshinone I in human colon cancer Colo 205 cells. *Int. J. Mol. Med.* **2008**, *22*, 613–618; c) Liu, J. J.; Liu, W. D.; Yang, H. Z.; Zhang, Y.; Fang, Z. G.; Liu, P. Q.; Lin, D. J.; Xiao, R. Z.; Hu, Y.; Wang, C. Z. Inactivation of PI3k/Akt signaling pathway and activation of caspase-3 are involved in tanshinone I-induced apoptosis in myeloid leukemia cells *in vitro*. *Ann. Hematol.* **2010**, *89*, 1089–1097.

8. Yu, H.; Subedi, R. K.; Nepal, P. R.; Kim, Y. G.; Choi, H.-K. Enhancement of solubility and dissolution rate of cryptotanshinone, tanshinone I and tanshinone IIA extracted from *Salvia miltiorrhiza*. *Arch. Pharm. Res.* **2012**, *35*, 1457-1464.

9. a) Park, E. J.; Ji, H. Y.; Kim, N. J.; Song, W. Y.; Kim, Y. H.; Kim, Y. C.; Sohn, D. H.; Lee, H. S. Simultaneous determination of tanshinone I, dihydrotanshinone I, tanshinone IIA and cryptotanshinone in rat plasma by liquid chromatography–tandem mass spectrometry: Application to a pharmacokinetic study of a standardized fraction of Salvia miltiorrhiza, PF2401-SF. *Biomed. Chromatogr.* **2008**, *22*, 548–555; b) Liu, Y.; Li, X.; Li, Y.; Wang, L.; Xue, M. Simultaneous determination of danshensu, rosmarinic acid, cryptotanshinone, tanshinone IIA, tanshinone I and dihydrotanshinone I by liquid chromatographic–mass spectrometry and the application to pharmacokinetics in rats. *J. Pharm. Biomed. Anal.* **2010**, *53*, 698–704.

10. a) Qin, Y. L. Preparation of Tanshinone I Derivatives for Pharmaceutical Use. CN Patent 1837200A, 2006; b) Xu, W.; Jiang, C.; Yang, F.; Shen, X.; Li, R.; Xue, D. Preparation of Tanshinone Derivatives as Anti-Tumor Agents. CN Patent 103288916, 2013; c) Rong, F.; Xu, R. Z.; Xie, F. W.; Lai, H. X. 2-Alkyl or -Aryl-Substituted

Tanshinone Derivatives, and Preparation Method and Application Thereof. U.S. Patent 201403336249 A1, 2014; d) Luan, D.; Qin, L.; Luan, S. Tanshinone Derivative Useful in Treatment of Various Diseases and Its Preparation. CN Patent 105884857, 2016; e) Jiao, M.; Ding, C.; Zhang, A. Preparation of 2-aryl derivatives of tanshinone I through a palladium-catalyzed C_{sp2}–H activation/arylation approach. *Tetrahedron Lett.* **2015**, *56*, 2799–2802; f) Wang, D.; Zhang, W.; Wang, T.; Li, N.; Mu, H.; Zhang, J.; Duan, J. Unveiling the mode of action of two antibacterial tanshinone derivatives. *Int. J. Mol. Sci.* **2015**, *16*, 17668-17681

11. a) Jin, H.; Li, H.; Mao, S.; Ma, W.; Chen, Y.; Liu, S. Tanshinone I Derivatives, Synthetic Method and Antitumor Application. CN Patent 102702302 A, 2012; b) Jiao, M.; Ding, C; Zhang, A. Facile construction of 3-hydroxyphenanthrene-1,4-diones Using a tandem three-step reaction sequence as key intermediates to tanshinone I and its 4-demethylated analogues. *Tetrahedron* **2014**, *70*, 2976-2981.

12. Yin, P. Synthesis, Characterization and Biological Activities of Tanshinone-Imidazole Derivatives. Master Dissertation, Guangdong Pharmaceutical College, Guangdong, China, 2011.

13. Yang, B.; Qian, M.; Qin, G.; Chen Z. Studies on the active principles of Dan-Shen V: isolation and structures of Przewaquinone A and Przewaquinone B. *Acta Pharm. Sin.* **1981**, *16*, 837-841.

14. a) da Silva Junior, E. N.; de Souza, M. C. B. V.; Pinto, A. V.; Pinto, M. C. F. R.; Goulart, M. O. F.; Pessoa, C.; Costa-Lotufo, L.; Montenegro, R. C.; Moraes, M. O.; Ferreira, V. F. Synthesis and potent antitumor activity of new arylamino derivatives

of nor-*β*-lapachone and nor-β-lapachone. *Bioorg. Med. Chem.* **2007**, *15*, 7035–7041; b) da Silva Jr, E. N.; de Deus, C. F.; Cavalcanti, B. C.; Pessoa, C.; Costa-Lotufo, L. V.; Montenegro, R. C.; de Moraes, M. O.; Pinto Mdo, C.; de Simone, C. A.; Ferreira, V. F.; Goulart, M. O.; Andrade, C. K.; Pinto, A. V. *J. Med. Chem.* **2010**, 53, 504–508.

15. Glazunov, V. P.; Berdyshev, D. V.; Yakubovskaya, A. Ya.; Pokhilo, N. D. Chemistry of naphthazarin derivatives 13: Conformational analysis of 3-(alk-1-enyl)-2-hydroxy-1,4-naphthoquinones by quantum chemistry methods. *Russ. Chem. Bull. Int. Ed.* **2006**, *55*, 1729-1736.

16. Morrell, A.; Antony, S.; Kohlhagen, G.; Pommier, Y.; Cushman, M. A. Systematic study of nitrated indenoisoquinolines reveals a potent topoisomerase I inhibitor. *J. Med. Chem.* **2006**, *49*, 7740–7753.

17. González, C.; Guitián, E.; Castedo, L. Synthesis of phenanthridones, quinolinequinones and 7-azasteroids. *Tetrahedron* **1999**, *55*, 5195-5206.

18. a) Vogel, G. H. Determination of Solubility by Hyphenated HPLC Methods. In *Drug Discovery and Evaluation: Safety and Pharmacokinetics Assay*; Vogel, H. G., Maas, J., Hock, F. J., Mayer, D., Eds.; Springer: New York, 2006; pp 400-402; b) Kiselev, E.; DeGuire, S.; Morrell, A.; Agama, K.; Dexheimer, T. S.; Pommier, Y.; Cushman, M. 7-Azaindenoisoquinolines as topoisomerase I inhibitors and potential anticancer agents. *J. Med. Chem.* **2011**, *54*, 6106-6116.

19. Chow, S. C.; Weis, M.; Kass, G. E. N.; Holmstrom, T. H.; Eriksson, J. E.; Orrenius S. Involvement of multiple proteases during Fas-mediated apoptosis in T lymphocytes. *FEBS Lett.* **1995**, *364*, 134-138.

Table of Contents Graphic

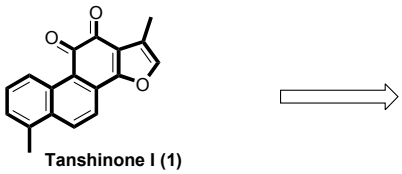

Tanshinone I (1)

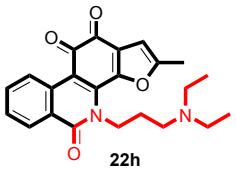

22h

- Poor aqueous solubility (<10^{-4} mg/mL)
- Instability in liver microsomes ($T_{1/2}$ = 2~6 min)
- Low bioavailability (F = ~0%)
- Moderate anticancer potency (IC_{50} = 4~6 μM)

- Improved aqueous solubility (15.7 mg/mL)
- Increased stability in liver microsomes ($T_{1/2}$ = 50~90 min)
- Improved bioavailability (*F* = 21%)
- Enhanced anticancer potency (IC_{50} = 0.12~0.33 μM)
- Significantly suppressing colon cancer xenograft tumor growth *in vivo* at 10.0 mg/kg